Desalination 629 (2026) 120098

Contents lists available at ScienceDirect

Desalination

journal homepage: www.elsevier.com/locate/desal

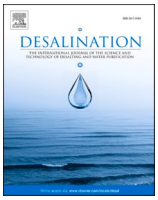

Advances in capacitive deionization for selective lithium recovery from brines: Mechanisms, strategies, and future perspectives

Hanwei Yu [a], Sherub Phuntsho [a], Gayathri Naidu [a], Mohsen Askari [a], Ho Kyong Shon [a,*]

[a] ARC Research Hub for Nutrients in a Circular Economy, Center for Technology in Water and Wastewater, School of Civil and Environmental Engineering, Faculty of Engineering and IT, University of Technology Sydney, P.O. Box 123, Broadway, NSW, 2007, Australia

HIGHLIGHTS

- Systematic review of CDI for selective lithium recovery from brines
- Compares CDI, MCDI, FCDI, and HCDI for lithium extraction
- Summarizes electrode design and interface modification strategies
- Evaluates metrics for selectivity, capacity, energy, and stability
- Proposes standardization and future directions for CDI research

GRAPHICAL ABSTRACT

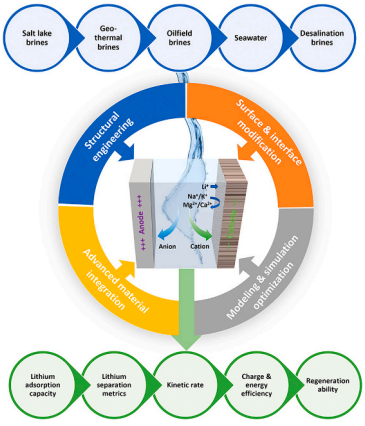

ARTICLE INFO

Keywords:
Lithium recovery
Capacitive deionization
Brines
Electrode modification
Electrosorption

ABSTRACT

The growing global demand for lithium, fueled by the expansion of electric vehicles and energy storage systems, calls for efficient and sustainable extraction technologies. Capacitive deionization (CDI) is emerging as a promising electrochemical method for lithium recovery from diverse aqueous sources, including low-grade brines, geothermal waters, and industrial effluents. By applying a low-voltage electric field, CDI captures lithium ions either through electrosorption onto porous electrodes or via intercalation into redox-active materials. Compared to conventional separation technologies, CDI offers distinct advantages such as low energy consumption, mild operating conditions, rapid adsorption kinetics, and scalable modular design. This review systematically summarizes recent advancements in CDI-based lithium extraction with a focus on research methodology. Key research strategies are categorized into four domains: structural engineering of electrodes, surface and interface modification, advanced material integration, and machine learning and simulation. Applications across various source solutions are discussed, and standard performance metrics such as adsorption capacity, selectivity, energy consumption, and cycling stability are outlined. The review concludes by identifying critical challenges and proposing future research directions that emphasize multifunctional electrode design,

* Corresponding author.
E-mail address: Hokyong.Shon-1@uts.edu.au (H.K. Shon).

https://doi.org/10.1016/j.desal.2026.120098
Received 17 March 2026; Accepted 19 March 2026
Available online 20 March 2026

scalable fabrication, and data-driven material discovery. This work offers comprehensive guidance for advancing CDI technologies toward practical and sustainable lithium recovery.

1. Introduction

The global transition toward renewable energy, electric vehicles (EVs), and portable electronics has drastically increased the demand for lithium, a critical component of lithium-ion batteries [1]. According to recent projections, global lithium demand may exceed supply as early as 2030, driven by aggressive decarbonization targets and battery market expansion [2]. While traditional lithium sources such as pegmatites and high-grade salt lakes continue to dominate global production, they are geographically concentrated, capital-intensive, and environmentally disruptive [3–5]. Consequently, the development of alternative lithium sources, such as seawater and low-grade brines, has garnered significant attention [6–12].

However, recovering lithium from these dilute and complex aqueous matrices poses critical technical and economic challenges. The low lithium concentration, e.g., ~0.2 mg/L in seawater and < 100 mg/L in many geothermal brines, and the presence of competitive ions such as Na^+, Mg^{2+}, K^+, and Ca^{2+} at orders-of-magnitude higher concentrations, limit the effectiveness of conventional separation methods such as precipitation, solvent extraction, and membrane filtration [1,9,13]. These limitations call for highly selective, energy-efficient, and regenerable lithium extraction technologies.

In recent years, capacitive deionization (CDI) is emerging as a promising electrochemical technique for lithium recovery [14]. CDI operates at low voltages and removes ions from water by electrosorption onto porous electrodes or via intercalation into redox-active materials [14–16]. Compared to traditional separation technologies, CDI offers several advantages, including low energy consumption, mild operating conditions, rapid adsorption and desorption kinetics, material regeneration ability, and modular scalability [17–19]. Despite substantial progress over the past decade, CDI for lithium recovery remains in its developmental stage, with challenges in achieving high selectivity and scalability. Conventional CDI electrodes, typically based on activated carbon, lack inherent lithium selectivity [20]. To address these challenges, recent research has explored a diverse array of electrode engineering strategies, including surface and interface modification, functional material integration, membrane-based systems, and theory-guided material screening.

Several recent reviews have summarized lithium extraction technologies from aqueous resources, including membrane-based, adsorption-based, and electrochemical approaches, in which CDI is typically mentioned as one of several emerging techniques [11,21–26]. Other reviews have focused on CDI technology itself, emphasizing electrode materials, system configurations, and water treatment applications [27–30]. However, the specific application of CDI for lithium recovery has generally received limited dedicated discussion. With the rapid growth of studies on CDI-based lithium recovery in recent years, the literature has become increasingly fragmented in terms of materials design, system configurations, feed compositions, and evaluation metrics. A focused synthesis is therefore needed to consolidate recent advances and provide a clearer framework for this emerging research direction. This review aims to provide a systematic and research-method-oriented review of recent advancements in CDI for lithium recovery from brines and other aqueous solutions. By organizing the field along methodological lines, this review seeks to offer actionable insights for researchers, comparative analysis across CDI configurations, and design guidelines for high-performance lithium recovery systems.

2. Capacitive deionization technologies for lithium recovery

2.1. Basic principles of CDI and extended systems

CDI is an emerging electrochemical separation technique that removes charged species from saline water using a low-voltage electric field, and is increasingly recognized as a promising approach for lithium recovery from dilute brine solutions [15,22,31–35]. This technology was initially conceived by Blair and Murphy in 1960, and the term "CDI" was first put forward by Farmer et al. in 1996 [36]. CDI operates under low voltages (typically ≤1.5 V), driving cations and anions toward oppositely charged porous electrodes with high specific surface areas. Upon polarization reversal, the temporarily adsorbed ions are released back into the bulk solution, completing the regeneration cycle. [37]. In its conventional form, CDI employs a pair of porous electrodes to adsorb cations and anions onto oppositely charged surfaces through the formation of electric double layers (EDLs). Upon voltage reversal or discharge, the adsorbed ions are released, allowing for electrode regeneration and target ion recovery [38–40]. To further enhance the ion-removal performance, more novel CDI cell architectures, including membrane CDI (MCDI) [41–43], flow-electrode CDI (FCDI) [44,45], and hybrid CDI (HCDI) [46,47], have been investigated in recent years, as presented in Fig. 1.

2.1.1. Membrane CDI (MCDI)

MCDI is an advanced configuration of classical CDI, in which ion-exchange membranes (IEMs) or ion-selective membranes (ISMs) are incorporated between oppositely charged electrodes. The presence of these membranes mitigates co-ion expulsion, suppresses anode oxidation, lowers energy consumption, and enhances both ion adsorption capacity and selectivity [48–50]. MCDI was first applied to wastewater desalination in 2006 by Lee et al., targeting effluents from a thermal power plant [51]. Beyond investigating operational modes and performance of ion removal [52–57], researchers attempted to expand its application to selective recovery of target ions from aqueous solutions [41,58]. Notably, MCDI demonstrates high separation efficiency and low energy consumption when dealing with low-concentration solutions (≤ 20 mM), making it particularly attractive for resource recovery from dilute streams. In recent years, the progress of MCDI studies is concentrated in membrane fabrication [59,60], operation optimization [55,61], cell structure design [62,63], and application development [64].

2.1.2. Flow-electrode CDI (FCDI)

FCDI was first introduced by Jeon et al. in 2013 for seawater desalination [65], building upon the concept of the flow electrode put forward by Kastening et al. in 1997 [66]. Among various CDI architectures, FCDI represents a distinct configuration in which the stationary solid electrodes are replaced by continuously circulating slurry-based electrodes, which enables uninterrupted operation and theoretically unlimited ion removal capacity, making it well-suited for continuous desalination processes [67,68]. Similar to the conventional CDI electrodes, the active phase of the flow electrode primarily comprises carbon-based or battery-type materials, which serve as ion adsorption media. In addition to the active material, flow electrodes also contain supporting electrolytes and conductive additives to ensure sufficient charge transport and rheological stability [69,70]. The applications of FCDI range from seawater desalination [71], water softening [72], control of toxic chemicals and heavy metals [73], to resource and nutrient recovery [74].

2.1.3. Hybrid CDI (HCDI)

HCDI, proposed by Lee et al. in 2014, is a modified CDI configuration inspired by electrochemical energy storage systems [75]. In this design, one of the capacitive electrodes is replaced with a faradaic intercalation-type electrode, enabling selective and reversible recovery of target ions through redox-driven insertion processes [38,76]. The incorporation of a battery-type electrode in HCDI not only enhances ion selectivity but also significantly increases the overall ion storage capacity. This improvement arises from the dual ion storage mechanisms: electrostatic adsorption on the electrode surface and faradaic intercalation into the crystal lattice of the electrode material via redox reactions [77]. An ideal electrode for HCDI should possess a high specific capacity, good electrical conductivity, and economic viability to facilitate scalable implementation, e.g., manganese oxides, titanium oxides, phosphates, chromates, and Prussian blue (PB) [78–80].

Different CDI architectures exhibit distinct advantages and limitations in terms of ion transport, charge efficiency, operational complexity, and scalability. A comparison of the main CDI configurations used for lithium recovery, including flow-by CDI, MCDI, FCDI, and HCDI, is summarized in Table 1.

Table 1
Comparison of CDI architectures for lithium recovery.

CDI architecture	Working principle	Advantages	Limitations
Flow-by CDI	Feed solution flows parallel to the electrode surface while ions are removed through electrosorption or intercalation	Simple cell configuration; low hydraulic resistance; easy system integration	Limited ion transport efficiency; lower salt removal rate compared with flow-through designs
MCDI	Ion-exchange membranes are placed in front of electrodes to suppress co-ion expulsion and improve charge efficiency	Improved charge efficiency; enhanced ion selectivity; reduced parasitic reactions	Increased system cost due to membranes; potential membrane fouling and additional resistance
FCDI	Suspended conductive particles serve as flowable electrodes, enabling continuous ion adsorption and regeneration	Continuous operation; high salt adsorption capacity; scalable for large-volume processing	Complex system design; slurry stability and pumping energy requirements
HCDI	Combines capacitive carbon electrodes with Faradaic or intercalation-type electrodes	High ion selectivity; improved lithium recovery efficiency; tunable electrochemical properties	Material stability and cycling durability challenges; more complex electrode fabrication

2.2. Lithium recovery mechanisms in CDI

Selective lithium recovery in CDI systems relies on multiple interrelated physicochemical mechanisms, which govern lithium transport, recognition, and retention at the electrode-electrolyte interface. These mechanisms can be broadly classified into two main categories: non-Faradaic processes, which involve electrostatic adsorption without charge transfer, and Faradaic processes, which entail redox reactions and ion intercalation, as schematically illustrated in Fig. 2. In conventional CDI systems, Li^+ is primarily adsorbed via non-Faradaic EDL formation on the porous carbon electrodes. This mechanism is energy-efficient but generally suffers from low selectivity and limited capacity

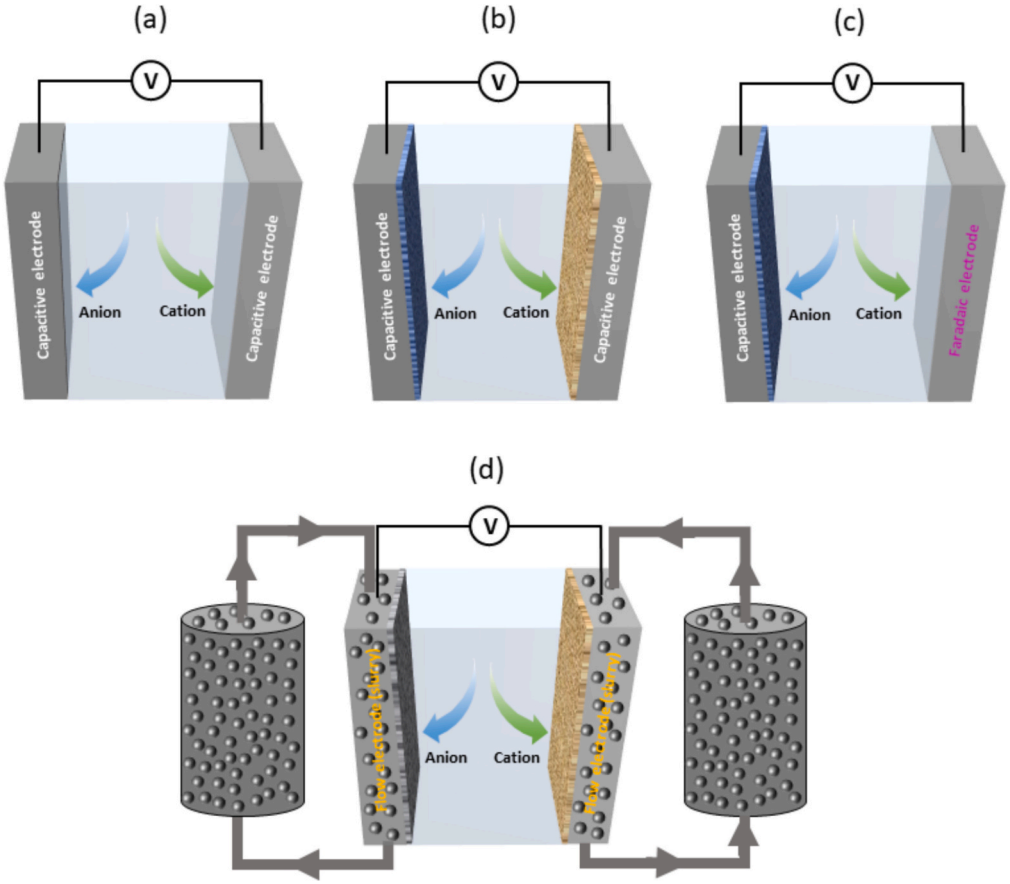

Fig. 1. Schematic illustrations of CDI cell architectures. a) Classical flow-by CDI, b) MCDI, c) HCDI, d) FCDI.

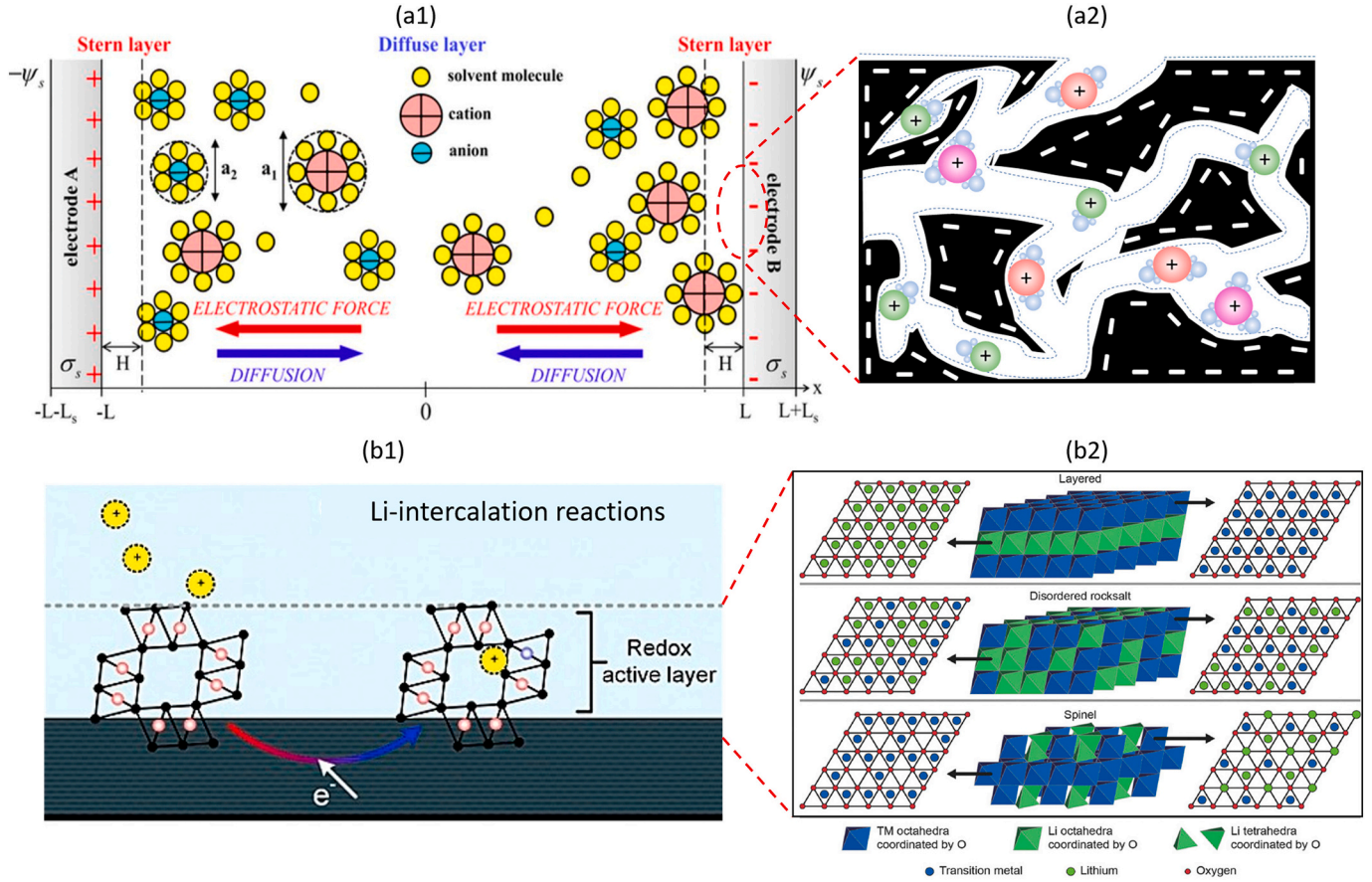

Fig. 2. Schematic illustration of Li extraction mechanisms in CDI systems. (a) non-Faradaic ion electrosorption mechanisms, where lithium ions are stored through electric double-layer (EDL) formation. (a1) Representation of a classical EDL structure formed between two planar electrodes, consisting of a compact Stern layer and a diffuse layer. The electrostatic attraction between charged electrodes and counter-ions governs ion accumulation, while diffusion controls ion transport within the electrolyte. (a2) Magnified view of ion electrosorption within the microporous carbon network, where hydrated cations are adsorbed. (b) Faradaic Li intercalation mechanisms, where Li ions are captured via redox reactions and intercalation into redox-active crystal frameworks. (b1) Li-intercalation process in a Faradaic electrode. (b2) Li occupancy within the vacant sites of various intercalation-type crystal structures. Fig. (a1) obtained from [89] with copyright permission from IOP Publishing. Fig. (b1) obtained from [90] with copyright permission from Elsevier. Fig. (b2) obtained from [91] with copyright permission from John Wiley and Sons.

due to non-specific interactions with coexisting ions [18,44,81,82].

Lithium selectivity under non-Faradaic conditions is primarily influenced by ionic hydration and structural accessibility. Fig. 3 illustrates the bare and hydrated ionic radius of Li and its main competitors in natural water resources. Ions with smaller hydrated radii are more likely to access microporous regions and active sites within electrode structures. In contrast, ions with larger hydration shells, such as Mg^{2+} and Ca^{2+}, are sterically excluded, especially under size-confining conditions [83–85]. This size-based discrimination becomes particularly effective when the pore distribution of the electrode is engineered with a

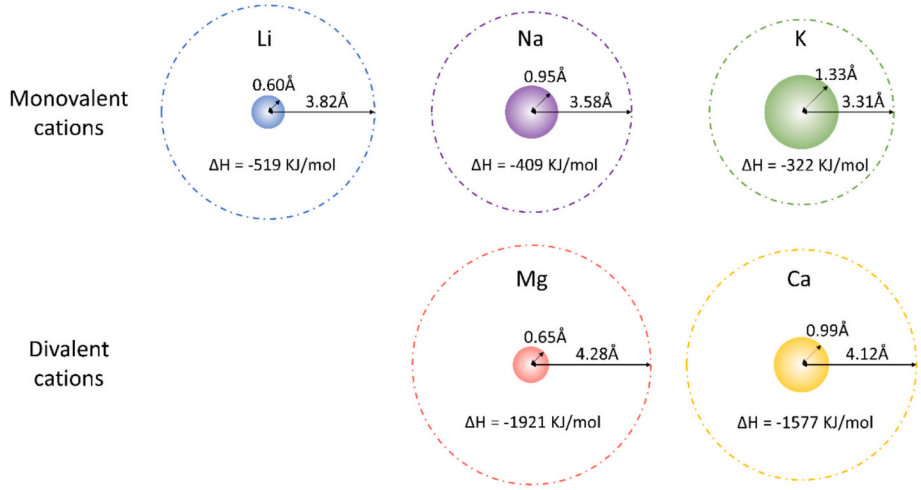

Fig. 3. Bare and hydrated ionic radius of Li, Na, K, Mg, and Ca and their hydration enthalpy. Figure obtained from [19] with copyright permission from Elsevier.

high proportion of micropores [86]. Moreover, ion valence plays a dual role: although divalent ions may have stronger electrostatic interactions, their higher hydration energy and limited mobility often result in lower uptake compared to monovalent lithium ions under identical conditions [87,88]. These structural and physicochemical parameters, including hydrated radius, valence, and ion–pore compatibility, collectively define the non-Faradaic selectivity behavior observed in carbon-based or hybrid electrodes.

Selective MCDI enhances non-Faradaic selectivity by introducing monovalent or Li-selective membranes, which act as size- and charge-based sieves against interfering ions and are well effective in complex mixtures with extreme ion ratios [17,19,60,92]. Some electrode surfaces are functionalized with chelating ligands or ion-imprinted polymers that exhibit specific affinity for Li^+ or competing cations, such as crown ethers [93,94], or sulfonic groups [95,96]. These provide additional selectivity through coordination chemistry. Strategies such as constructing vertically aligned channels or embedding active materials within conductive matrices, e.g., rGO, CNTs, reduce ion diffusion barriers and accelerate lithium transport [32,97–101]. These structural optimizations contribute to faster kinetics and improved separation performance., and the mechanisms are schematically illustrated in Fig. 4.

Advanced lithium-selective electrodes, such as $LiCoMnO_4$ [107], $LiFePO_4$ [108], and $Li_3V_2(PO_4)_3$ [109], function via redox-mediated lithium intercalation or conversion reactions. These Faradaic processes provide greater selectivity and capacity by leveraging crystal structures with favorable lithium diffusion pathways and binding energies [90,110,111]. Lithium-ion sieves (LIS) exhibit strong lithium preference due to their narrow interlayer spacings and memory effect, which allows for selective Li^+–H^+ exchange [1,99,112]. This mechanism is particularly effective at excluding multivalent ions based on steric hindrance and hydration energy differences.

In most advanced CDI systems, these mechanisms do not operate in isolation but synergistically. For example, a typical HCDI device may simultaneously leverage Faradaic intercalation, surface functionalization, and membrane selectivity to enhance both lithium capacity and separation factor. This integrated approach is increasingly emphasized in recent studies [97,113–115], where systems are specifically designed

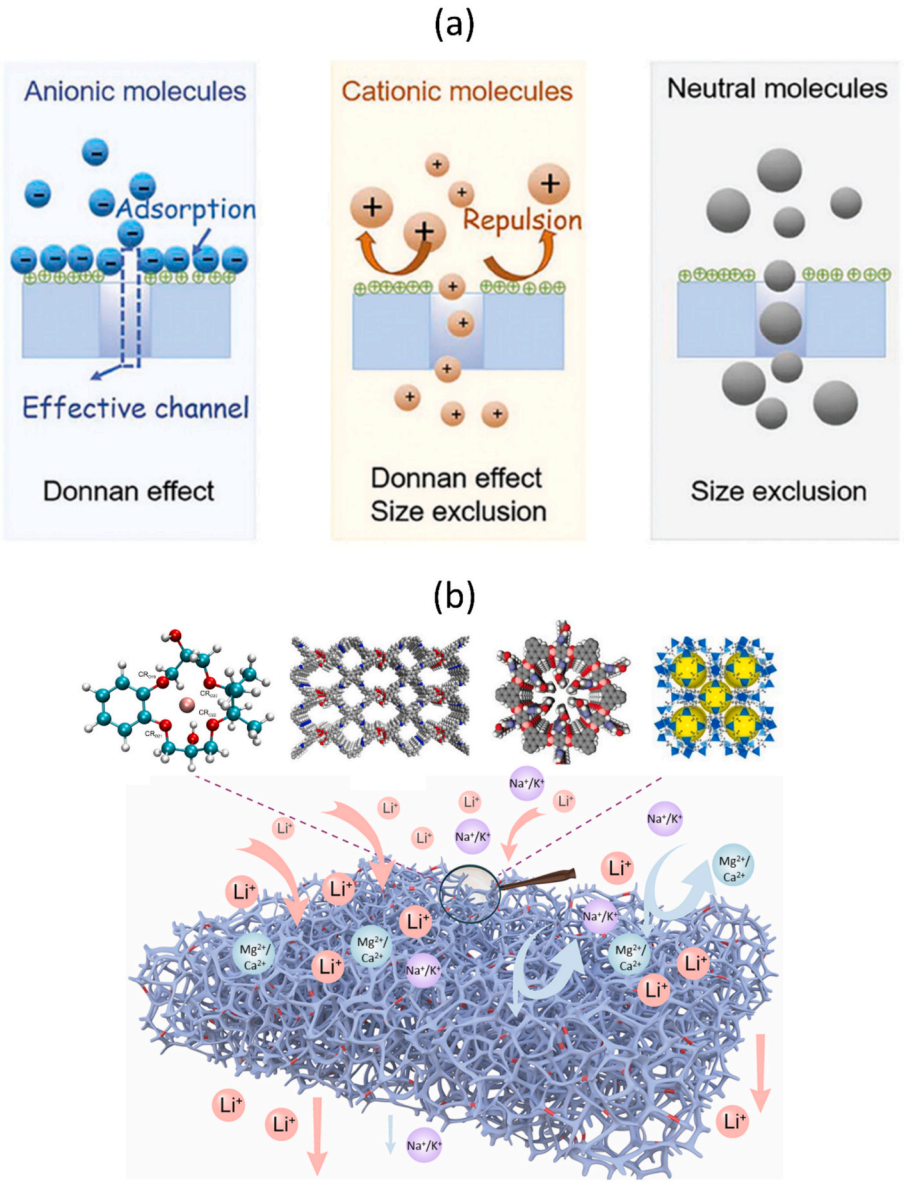

Fig. 4. Selectivity enhancement mechanisms in MCDI systems through (a) membrane-based ion discrimination and (b) surface functionalization. Figure (a) obtained from [102] with copyright permission from Royal Society of Chemistry. Figure (b) obtained and edited from [103–106] with copyright permission from Elsevier.

to combine complementary mechanisms for enhanced performance. Such multi-mechanism configurations enable the simultaneous benefits of high capacity, fast kinetics, and strong ionic discrimination. A clear understanding of these interactions is thus essential for the rational design of next-generation CDI materials and systems tailored for lithium extraction from diverse aqueous matrices.

3. Strategies for enhancing lithium recovery in CDI systems

While CDI offers a technically simple and energy-efficient platform for lithium extraction, its real-world application faces several challenges, notably the low lithium selectivity in the presence of competing cations and the degradation of electrode materials over multiple cycles. To address these issues, researchers have developed a wide range of strategies targeting material design, electrode architecture, interfacial chemistry, and system-level optimization. This section systematically categorizes recent advances in CDI-based lithium recovery according to research strategies, including structural engineering of electrodes, surface and interface modification, functional material integration, electrode screening, polymer and biomass-derived approaches, and simulation-guided material development [116,117].

3.1. Structural engineering of electrodes

Electrode structure plays a critical role in dictating ion transport kinetics, adsorption capacity, and regeneration efficiency in CDI systems. Strategies such as nanostructure design, aligned ion pathways, flexible substrates, and hierarchical porosity collectively contribute to improving lithium adsorption kinetics, selectivity, and cycling durability.

Architectural optimization at the micro- and nano-scale significantly enhances lithium ion accessibility and minimizes diffusion resistance. One common approach involves constructing one-dimensional nanostructures, e.g., nanorods or nanowire, that offer direct lithium ion transport pathways. For example, in-situ growth of $LiMn_2O_4$ nanorods on flexible carbon cloth ($LiMn_2O_4$@CC) reconciles the trade-off between capacity, conductivity, and porosity, achieving a high adsorption capacity of 37.7 mg/g and excellent Li^+/Mg^{2+} selectivity of 804.6 [118]. In addition to spinel-type lithium manganese oxides, other lithium intercalation materials and battery materials, including layered transition-metal oxides and layered oxides such as olivine $LiFePO_4$ and $Li(NiCoMn)O_2$ (NCM) have also attracted increasing attention as CDI electrodes for lithium extraction. $LiFePO_4$, widely used in lithium-ion batteries, possesses a stable olivine framework that enables reversible Li^+ intercalation/deintercalation with good structural stability and cycling durability [119–122]. Structural engineering strategies, including nanoscale particle design, conductive framework integration, and hierarchical porous architectures, have been applied to these materials to enhance lithium ion transport kinetics and electrode stability in electrochemical lithium recovery systems. Three-dimensional porous structures, including hollow nanocubes [107], vertically aligned graphene-based frameworks [97], hydrogels [123,124], and carbon aerogels [125], further increase the specific surface area and provide hierarchical pore networks. Representative examples of one-, two-, and three-dimensional electrode architectures are illustrated in Fig. 5. Flexible current collectors are another focus of structural engineering. Electrodes supported on carbon cloth or conductive textiles show better mechanical stability, higher areal capacitance, and scalable integration potential. Compared with rigid Ti-based substrates, flexible carbon cloth improves conductivity and lithium diffusion rate by several orders of magnitude, as demonstrated in the $LiMn_2O_4$@CC system [118].

Overall, structural engineering strategies primarily address mass transfer limitations and diffusion resistance in CDI electrodes. By constructing ordered ion transport pathways, hierarchical porous structures, and flexible conductive frameworks, these approaches improve lithium ion accessibility, accelerate ion diffusion, and enhance electrode stability during repeated adsorption-desorption cycles.

3.2. Surface and interface modification

Surface and interfacial properties of electrodes profoundly influence ion recognition, selectivity, charge transfer, and long-term electrochemical stability in CDI systems. Rational surface modification strategies have been widely adopted to tailor electrode–electrolyte interfaces for enhanced lithium recovery. The main strategies include elemental doping, surface coating, and interfacial modification, as schematically illustrated in Fig. 6.

One of the most widely explored strategies is elemental doping, such as Al, Zn, La, B, and N, to modulate the electronic structure and lattice parameters of lithium-selective materials. For instance, Al-doped $LiMn_2O_4$ demonstrated a reduced lattice constant, which led to a higher Li^+ diffusion coefficient and intercalation energy difference between Li^+ and Na^+. As a result, it achieved a selectivity of 1653.8 for Li^+/Na^+ and 434.9 for Li^+/Mg^{2+} in synthetic brine, with a lithium adsorption capacity of 21.7 mg/g [126]. Similarly, boron-doped $H_{1.6}Mn_{1.6}O_4$ significantly suppressed Jahn–Teller distortion and Mn dissolution while enhancing Li^+/Na^+ selectivity to 1211.68, owing to the B—O bond-induced stabilization and lattice contraction [113]. La-doping in lithium manganese oxide (La-LMO) has also been used to reduce Mn dissolution and improve electrochemical cycling stability. When encapsulated with graphene oxide (GO), the La-LMO composite exhibited a Li^+ capacity of 1.33 mmol g^{-1} and a Li^+/Mg^{2+} separation factor of 126, demonstrating the dual role of La doping in suppressing phase distortion and promoting structural rigidity [127].

In addition to bulk doping, surface coatings have been developed to mitigate structural degradation. For example, a thin layer of amorphous AlF_3 was deposited on $LiMn_2O_4$ spheres to prevent Mn leaching and phase transformation during lithium cycling. This AlF_3 coating not only enhanced surface stability but also enabled a Li^+ capacity of 31.5 mg/g and a selectivity factor of 7.66 for Li^+/Mg^{2+} [128]. Surface functionalization using chelation ligands or ion-imprinted polymers has also shown promising results. For example, an imprinted CDI electrode

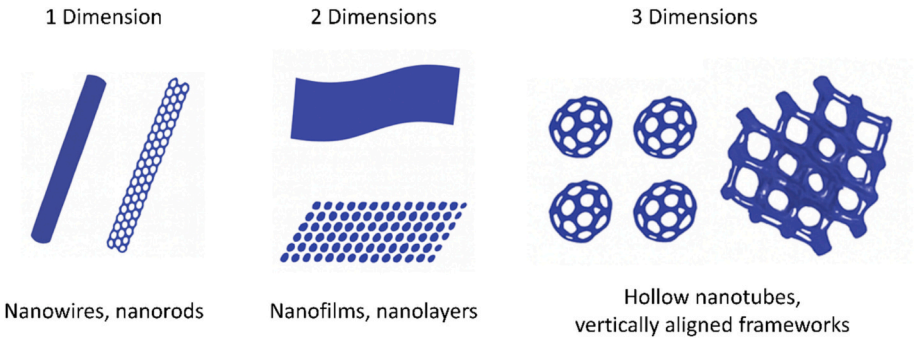

Fig. 5. Schematic illustration of one-, two-, and three-dimensional nanostructures.

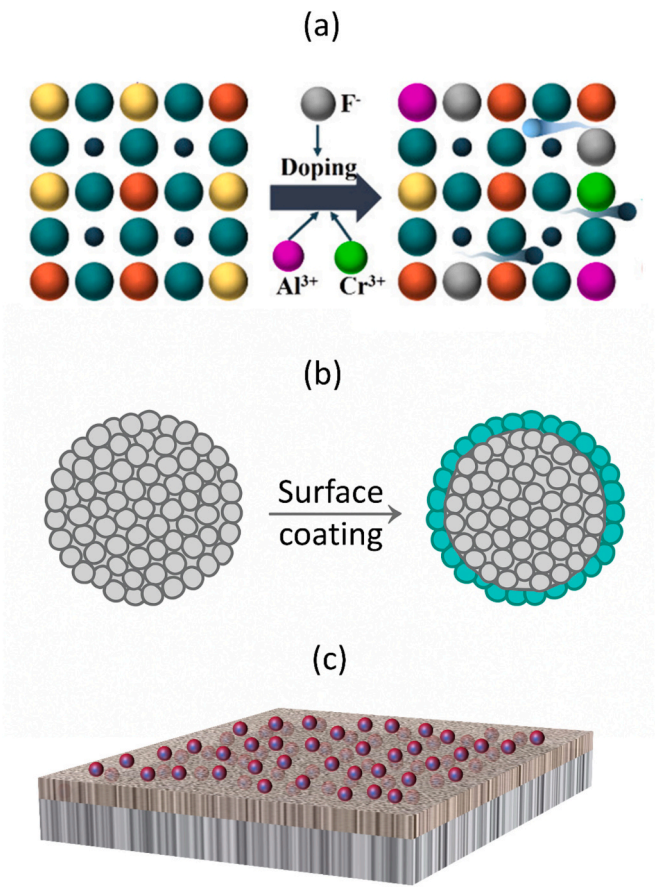

Fig. 6. Schematic illustration of surface and interface modification strategies for CDI electrodes, (a) element doping, (b) surface coating, (c) surface and interface modification. Figure (a) obtained from [130] with copyright permission from ACS Publications.

incorporating dibenzo-14-crown-4 ether and polypyrrole achieved lithium adsorption capacities of 2047.71 μmol/g in acidic conditions, with excellent selectivity over Na^+, K^+, Mg^{2+}, and Al^{3+} [129].

Interface modification via polymer coatings or membrane layers is another effective approach to improve ion selectivity and capacity [131,132]. For instance, layer-by-layer deposited PAH/PSS functional membranes were integrated with FCDI systems to convert a divalent-preferring cation exchange membrane into a monovalent-selective interface [132]. Similarly, selective lithium capture was enhanced by coupling Nafion membranes with $LiMn_2O_4$-coated surfaces, enabling selective MCDI devices to effectively separate Li^+ from concentrated Mg^{2+} environments with high charge efficiency [32]. Additionally, modifying electrode wettability and interfacial hydrophilicity through incorporation of graphene oxide, bacterial cellulose, or oxygen vacancies has been proven effective for facilitating lithium adsorption/desorption dynamics [97,125,133]. Such modifications improve electrolyte penetration and lower interfacial impedance, thus enhancing ion accessibility and system responsiveness.

In summary, surface and interface modification strategies mainly target the limited ion selectivity and structural instability of lithium-selective materials in complex brine environments. Through doping, surface coating, and interfacial functionalization, these approaches regulate ion recognition behavior, suppress structural degradation, and improve the electrochemical stability of CDI electrodes.

3.3. Advanced material integration

To further improve lithium selectivity, capacity, and electrochemical stability in CDI systems, researchers have increasingly explored the incorporation of advanced functional materials into the electrode matrix. These materials, including metal–organic frameworks (MOFs), conductive carbon nanomaterials, Prussian Blue analogues (PBAs), and MXenes, provide tailored physical and chemical environments to enhance lithium ion transport, recognition, and adsorption.

One promising class of materials is MOFs [134,135] and MOF-derived carbons [136–140]. A flow electrode based on ZIF-8/CNT composite exhibited exceptional conductivity and pore size compatibility with hydrated Li^+ ions, and achieved 2.3-fold higher deionization performance and significantly enhanced lithium selectivity over Na^+, Ni^{2+}, and Mn^{2+} ions [141]. $LiMn_2O_4$ nanoparticles in situ embedded in carbon networks derived from MOF led to a capacity of 3.5 mmol g^{-1} and a Li^+/Mg^{2+} separation factor of 24.5 [114].

Incorporating conductive carbon nanomaterials such as reduced graphene oxide (rGO) and CNT into active materials has become a prevalent strategy to boost electrical conductivity, structural integrity, and surface area. For instance, composites of Li_3VO_4/rGO, Li_2TiO_3/rGO, and λ-MnO_2/rGO have consistently outperformed their pure counterparts in terms of Li^+ adsorption capacity, cycling stability, and charge transfer efficiency [99–101]. The reduced graphene oxide (rGO) not only facilitates electron mobility but also prevents the aggregation of active nanoparticles, exposing more Li^+ adsorption sites. A representative study reported a CNT-strung $LiMn_2O_4$ (CNT-s-LMO) material with a net-like structure formed by threading CNTs through LMO particles. This unique configuration improved conductivity and enhanced electrochemical performance, achieving a Li^+/Mg^{2+} selectivity factor of 181 and 90% capacity retention after 100 cycles [98].

Prussian Blue (PB) and its analogues (PBAs) are another group of redox-active materials with open-framework crystal structures that allow for fast and reversible Li^+ intercalation. A CDI electrode composed of PB nanoparticles anchored on porous activated carbon delivered a high Li^+ electrosorption capacity of 24.42 mg/g, with 95.1% capacity retention after 50 cycles [111]. The synergistic interaction between PB's redox activity and the high conductivity of AC facilitated efficient charge transport and lithium intercalation. MXene materials, such as $Ti_3C_2T_x$, possess hydrophilic surfaces, metallic conductivity, and tunable interlayer spacing, which facilitate electrolyte wettability, accelerate electron transport, and provide ion diffusion pathways, thereby promoting efficient Li^+ transport and adsorption in CDI systems [142].

Overall, the integration of advanced functional materials provides synergistic improvements in conductivity, ion transport pathways, and lithium adsorption sites. By combining the advantages of multiple material components, these hybrid systems help overcome the intrinsic limitations of single-material electrodes and enable enhanced lithium recovery performance in CDI systems.

3.4. Modelling and simulation

The discovery and optimization of electrode materials for selective lithium recovery in CDI systems is a complex, multidimensional problem involving numerous variables: from material composition and morphology to electrochemical environment and operational parameters. Computational approaches have increasingly been used to support the rational design of CDI materials and systems for lithium recovery. However, their roles differ across methodologies. In the current literature, density functional theory (DFT), molecular dynamics (MD), and finite element simulations (FES) are used predominantly to elucidate ion adsorption, diffusion, and transport mechanisms, whereas recent machine learning (ML) studies have begun to demonstrate genuine predictive capability for performance estimation, parameter optimization, and accelerated material screening [6,143–146].

DFT calculations have played a central role in the rational screening of CDI electrode materials. By evaluating key properties such as adsorption energy, ionic diffusion barriers, and lattice deformation, DFT enables researchers to identify promising candidates before

experimental synthesis and analyze the mechanism of physical and chemical processes. For example, DFT studies of $Li_3V_2(PO_4)_3$ revealed that Li^+ has a lower diffusion energy barrier and smaller hydrated radius compared to Mg^{2+} and Ca^{2+}, explaining its superior selectivity in real brines [109]. Similarly, DFT has also been used to investigate the memory effect in lithium-ion sieve materials, such as H_2TiO_3, where Li^+/H^+ exchange occurs at narrowly confined lattice sites. Theoretical modelling demonstrated that Li^+ forms stronger hydrogen bonds and lower-energy adsorption configurations on the [111] facet compared to Na^+ and K^+, particularly when an external electric field is applied [147]. Beyond atomic-level insights, MD and finite FES offer complementary information on ion hydration, diffusion behavior, and macroscale transport phenomena in CDI systems [97,126].

More recently, ML has emerged as a complementary data-driven approach that enables predictive analysis of lithium adsorption performance and accelerated screening of electrode materials. By integrating large experimental datasets with material descriptors, operating parameters, and solution characteristics, ML models can identify key factors governing lithium selectivity and adsorption efficiency. Several recent studies have demonstrated that ML-based models can accurately predict lithium recovery performance and provide guidance for optimizing adsorbent design and operating conditions [6,143,145,146]. Compared with conventional mechanistic modelling, these data-driven approaches offer a promising pathway toward high-throughput screening and rational design of lithium-selective CDI electrodes. However, the application of ML in CDI-based lithium recovery remains at an early stage and is currently limited by data availability.

4. Source solutions and performance evaluation in CDI-based lithium recovery

Although CDI technology study for lithium recovery application has emerged as a trending research topic, the lack of standardization in feed solution selection and performance evaluation methods remains a major barrier to cross-study comparability, material benchmarking, and industrial translation. Researchers employ diverse feed compositions, ranging from simplified LiCl solution to complex natural brines, as well as inconsistent metrics to evaluate performance, making it difficult to fairly compare electrode materials or system architectures. This section presents a comprehensive and critical analysis of the feed solution types and performance metrics commonly employed in CDI-based lithium recovery studies. The influence of these choices on experimental outcomes is discussed, and standardized recommendations are proposed to enhance reproducibility, consistency, and reliability within the research community.

4.1. Feed solutions

CDI has shown versatility across a broad range of lithium-containing solutions. However, the effectiveness of CDI technologies for lithium recovery is highly dependent on the characteristics of the source solution, including lithium concentration, coexisting ion composition, and solution complexity. Different water sources, such as simplified brines, synthetic brines, natural brines including salt lakes, geothermal brines, oilfield brines, and seawater brines, present diverse challenges and opportunities for CDI-based lithium extraction. While synthetic systems offer high control for mechanism studies, real brine applications test the system's selectivity and long-term performance.

The ionic composition of these aqueous resources varies drastically across different origins. Seawater and desalination brine typically contain Li^+ in trace levels (< 2 mg/L), accompanied by abundant Na^+ and Mg^{2+} ions, whereas salt lakes and geothermal brines can exhibit Li^+ concentrations from sub-ppm levels up to several grams per litre, depending on local geochemical evolution. Fig. 7(a) summarizes the representative cation concentrations of Li, Na, K, Mg, Ca in seawater, desalination brine, salt-lake, geothermal, and oilfield brines, clearly

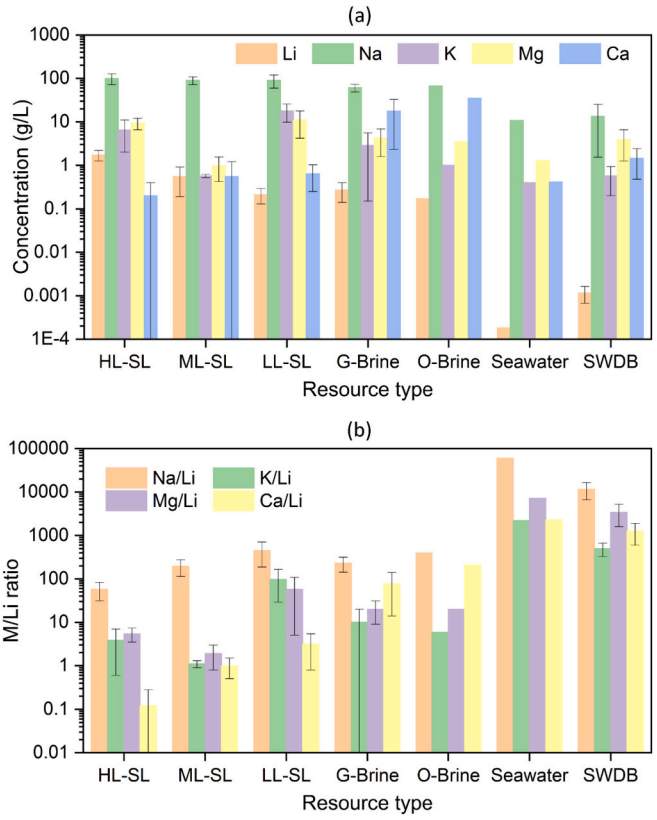

Fig. 7. Representative ionic composition and lithium selectivity challenge across different aqueous resources. (a) Major cation concentrations (Li^+, Na^+, K^+, Mg^{2+}, Ca^{2+}) for high-Li (HL-SL), medium-Li (ML-SL), and low-Li (LL-SL) salt lakes, geothermal brine (G-Brine), oilfield brine (O-Brine), seawater, and seawater-desalination brine (SWDB). (b) Corresponding M/Li concentration ratios (Na/Li, K/Li, Mg/Li, Ca/Li) derived from panel (a), illustrating the selectivity difficulty among resource types. The data for Figure (a) normalization is from [148–153].

illustrating the orders-of-magnitude differences in lithium content and the dominance of competing ions such as Na^+ and Mg^{2+}. Specifically, high-Li salt lakes (HL-SL) were represented by the Atacama and Zabuye salt lakes, exhibiting $Li^+ > 1$ g/*L*. *medium*-Li salt lakes (ML-SL) included the Hombre Muerto and Clayton Valley brines, characterized by intermediate Li^+ contents (0.3–1 g/L). Low-Li salt lakes (LL-SL) encompassed the Uyuni, Qarhan, Chott Djerid, Taijinar, Da Qaidam, Yiliping, Lungmu Co, and related brines, all with $Li^+ \leq 0.3$ g/L. Geothermal brines (G-Brine) were derived from Southern Tibet, Salton Sea, Cerro Prieto, and Cesano sources, while oilfield brines (O-Brine) were represented by the Smackover formation. The average and standard deviation of Li^+, Na^+, K^+, Mg^{2+}, and Ca^{2+} concentrations were calculated from the published data of these representative brines [148–153]. Fig. 7(b) illustrates the corresponding ionic ratios of Na/Li, K/Li, Mg/Li, Ca/Li.

4.1.1. Synthetic single-ion and binary solutions

Synthetic lithium-containing solutions, often composed of LiCl or LiOH with or without selected competing cations (e.g., Na^+, K^+, Mg^{2+}, Ca^{2+}), are widely used in laboratory-scale studies for initial evaluation of lithium adsorption capacity and electrode kinetics under idealized conditions. A representative selection of CDI studies utilizing single or binary feed electrolytes is presented in Table 2. In single-ion solution cases, lithium concentration can play a critical role in capacity achievement. For example, an MCDI cell using H_2TiO_3/rGO composite electrodes achieved a Li^+ adsorption capacity of 13.67 mg/g in a 69.4 mg LiCl solution [101]. In another study, Li_3VO_4/rGO electrodes exhibited the highest reported Li^+ adsorption capacity of approximately

Table 2
Representative CDI studies employing single and binary feed solutions for Li recovery. The table includes CDI cell architecture, electrode material, applied voltage, feed solution type, and reported lithium extraction performance.

Cell architecture	Electrode material	Applied voltage	Source solution	Li extraction performance	Ref.
Flow-by CDI	LVO/rGO	1.2 V	610.42 mg/L LiCl solution	LAC~39.53 mg/g, remained ~30.84 mg/g after 20 cycles	[100]
	λ-MnO_2/rGO	−0.9 to 0.7 V	423.9 mg/L LiCl solution	LAC~206 μmol/g, remained 75% after 30 cycles	[99]
MCDI	AC/ZIF-8	±1.0 V	Li/Na, Li/K, Li/Mg, Li/Ca binary solutions	ρ_{Na}^{Li}~3.08	[20]
	AC/ZIF-8-PDA	±0.5, ±1.0, ±1.5 V		ρ_{K}^{Li}~1.85	[19]
	AC/CB/PVDF	0.6 to 1.4 V	Li/Mg solution (500 mg/L of Li)	ρ_{Mg}^{Li}~2.95	[34]
	LMO/GA/PVA	0.1 to 2.0 V	50 mg/L LiOH solution	LAC~1.36 mg/g	[131]
FCDI	AC-LiCl slurry	1.2 V	1 to 100 mg/L LiCl solution	LiCl removal~85.7%	[160]
HCDI	LNMO/AC	−0.3 to 0.8 V	423.9 mg/L LiCl solution Li/Mg mixed solution	LAC~260 μmol/g ρ_{Mg}^{Li}~104	[157]
	LMO/AC	1.0 V	Binary solution (69.4 mg/L of Li)	LAC~0.35 μmol/g	[133]
	LMTO/AC/PVDF-EDA	1.23 V	LiCl solution	LAC~31.1 mg/g	[161]

39.53 mg/g in 610.42 mg/L LiCl solution [100].

Binary model systems incorporating Li ion with one competing cation are widely adopted to quantify pairwise ion selectivity. These systems are especially valuable for elucidating the competitive adsorption behavior and the role of ionic properties such as valence, hydrated radius, and dehydration energy in CDI processes. Reported selectivity values vary significantly across studies, depending on both the absolute concentrations and the molar ratio between Li^+ and the competing ion. Some studies adopt equimolar Li^+/M^{n+} ratios to isolate the intrinsic selectivity of electrode materials [19,20,31,154], whereas others vary the concentration ratio to simulate diverse brine conditions and stress-test selectivity under asymmetric competition [126,155]. For example, one investigation systematically altered the Li^+/Na^+ ratio (e.g., 3:17, 10:10, 17:3) while maintaining constant ionic strength, demonstrating that both lithium recovery and selectivity are strongly influenced by the relative abundance of competing ions [156]. Similarly, a study employing λ-MnO_2-based electrodes demonstrated that, at a fixed Li^+ concentration of 10 mM, increasing the Mg^{2+}/Li^+ ratio from 1:1 to 20:1 resulted in a monotonic increase in the Li^+/Mg^{2+} separation factor from 5.0 to 24.5 [114]. Other studies using $LiCoMnO_4$ nanotube [107] and $LiNi_{0.5}Mn_{1.5}O_4$ [157] electrodes observed a similar trend, reporting a substantial increase in Li^+/Mg^{2+} selectivity from 3 to 88.7 and from 5 to 104, respectively, as the Mg^{2+}/Li^+ ratio increased from 1 to 30, with Li^+ concentration held at 5 mM. A similar pattern was observed with HMO@ZIF-AC electrodes tested in Li^+/Na^+ binary mixtures. As the Na^+/Li^+ molar ratio increased from 1 to 96, the selectivity factor rose from 5.0 to 115.0 [158]. These findings collectively suggest that, contrary to conventional expectations, increasing the relative abundance of the competing cation, i.e., a higher M^{n+}/Li^+ ratio, can enhance the calculated selectivity factor. This counterintuitive trend can be partially attributed to the definition of the selectivity factor, which depends on the relative adsorption changes of Li^+ and the competing ion. When the concentration of the competing ion increases, its adsorption onto lithium-selective materials often remains strongly suppressed due to unfavorable hydration energy, steric constraints, or limited intercalation compatibility. As a result, the relative difference between Li^+ uptake and competing-ion adsorption becomes more pronounced, leading to a higher calculated selectivity factor even though the absolute lithium adsorption capacity may remain unchanged or only moderately affected. However, exceptions have also been reported. In a study investigating the effect of different Mg^{2+}/Li^+ ratios on the performance of the R-FCDI system, Ma et al. reported that, solutions with Mg/Li ratios of 10, 20, and 30 yielded non-monotonic selectivity trends, with corresponding separation factors of 4.67–15.93, 8.52–11.04, and 1.48–3.12, respectively [159].

4.1.2. Simulated and natural brines

To evaluate the practical feasibility of CDI systems for lithium recovery, many studies have moved beyond idealized binary and single-ion electrolytes to more complex brine compositions. These include laboratory-prepared synthetic brines, designed to mimic the ionic environment of typical salt lake or geothermal resources, as well as real brine samples collected directly from natural sources. Together, these solution types offer critical insight into the selectivity, robustness, and operational viability of CDI systems under conditions that more closely resemble industrial applications. Simulated brines are typically composed of lithium alongside a mixture of competing cations (e.g., Na^+, Mg^{2+}, K^+, Ca^{2+}) in concentration ratios representative of real sources. These solutions allow for controlled testing of selectivity mechanisms under high ionic strength, high Mg/Li ratios, and multivalent ion interference. A representative summary of key CDI performance outcomes using simulated brines is provided in Table 3. The table compiles major cation concentrations and corresponding Li^+ selectivity factors, highlighting the variation in CDI system types and brine formulations used across studies.

On the other hand, real brine samples provide the most rigorous assessment of system performance as these samples often exhibit complex and variable compositions. While such heterogeneity poses reproducibility challenges, it also validates CDI systems under realistic operating conditions. A representative summary of CDI studies using natural brines is provided in Table 4. The table lists the major cationic constituents and reported Li^+ selectivity factors for brines from salt lakes such as Dongtaijinaier, Tibet, Golmud, Zabuye, East-Taijinaier, and Lop Nor. Selectivity factors vary widely across samples, ranging from modest values, e.g., Li/Mg ≈ 2.0 in Lop Nor, to exceptionally high figures, e.g., Li/Mg ≈ 6307.2 in Golmud or Li/Na ≈ 513 in Zabuye, reflecting the combined influence of source composition, CDI system architecture, and electrode material design. These studies have shown that with appropriate electrode design, such as the use of spinel-structured materials, functional coatings, and composite architectures, CDI systems can achieve excellent selectivity even in real brines with complex ionic backgrounds [109,114,118,125,159,162–164].

4.2. Performance metrics and evaluation methods

Quantitative evaluation of lithium recovery performance is essential for comparing CDI systems, understanding adsorption mechanisms, and guiding the design of next-generation electrodes and cell architectures. The performance assessment of CDI-based lithium recovery systems critically depends on the selection and application of appropriate evaluation metrics. Due to the diversity of experimental conditions and reporting standards across studies, establishing consistent and comparable performance benchmarks remains a significant challenge. This

Table 3
Representative studies employing simulated brines with multi-cationic composition to evaluate the selectivity of CDI systems for lithium recovery. The table summarizes the major cation concentrations, CDI configuration, and reported selectivity performance. Selectivity factors (ρ) are defined as the ratio of Li^+ removal relative to competing cations.

Simulated brine type	Cation concentration (mg/L)					CDI type	CDI performance	Ref.
	Li	Na	K	Mg	Ca			
Geothermal brine	15.7	10,298	102	50	/	FCDI	ρ_{Na}^{Li}~141, ρ_{K}^{Li}~46	[165]
Salt Lake brine	162.97	5897.84	1870.13	2937.38	22.85	Flow-by CDI	ρ_{Na}^{Li}~38, ρ_{K}^{Li}~57, ρ_{Mg}^{Li}~41, ρ_{Ca}^{Li}~ 8	[99]
						HCDI	ρ_{Na}^{Li}~82, ρ_{K}^{Li}~58, ρ_{Mg}^{Li}~76, ρ_{Ca}^{Li}~ 10	[107]
Salar de Uyuni brine	34.7	–	–	–	–	Flow-by CDI	ρ_{Na}^{Li}~365, ρ_{K}^{Li}~298, ρ_{Mg}^{Li}~48, ρ_{Ca}^{Li}~ 115	[127]
	166.56	20,921	3128	3403	120.24	HCDI	ρ_{Na}^{Li}~782.3, ρ_{Na}^{Li}~707.4, ρ_{Na}^{Li}~449.2	[97]
Baqiancuo brine	5.52	2299	277.61	316.03	60.12			
Atacama brine	145.74	7587	1798.6	97.24	308.62			
West Taijnar Salt Lake brine	300	102,400	8500	15,400	200	HCDI	ρ_{Na}^{Li}~1653.8, ρ_{Mg}^{Li}~434.9	[126]
	241.62	100,843	15,582	15,083	3541	HCDI	ρ_{Na}^{Li}~1212, ρ_{K}^{Li}~1292, ρ_{Mg}^{Li}~1352, ρ_{Ca}^{Li}~783	[113]
	220	82,600	6900	13,200	310	HCDI	High Li^+ selectivity; negligible uptake of Na^+, K^+, Mg^{2+}, Ca^{2+}	[166]
Simulated Brine	162.96	5900	1869	2938	22.85	MCDI	ρ_{Na}^{Li}~5.74, ρ_{K}^{Li}~40, ρ_{Mg}^{Li}~5.25, ρ_{Ca}^{Li}~5.48	[167]
	1500	76,000	18,500	9600	310	HCDI	ρ_{Na}^{Li}~11, ρ_{K}^{Li}~47, ρ_{Mg}^{Li}~167, ρ_{Ca}^{Li}~334	[157]
	2	2000	500	1000	500	MCDI	ρ_{Na}^{Li}~568, ρ_{K}^{Li}~643, ρ_{Mg}^{Li}~505, ρ_{Ca}^{Li}~ 840	[115]
	34.7	115	–	121.6	–	CDI-RFB hybrid module	ρ_{Na}^{Li}~15.25, ρ_{Mg}^{Li}~57.7	[154]
	150	–	–	–	–	MCDI	ρ_{Na}^{Li}~2.85, ρ_{K}^{Li}~1.98, ρ_{Mg}^{Li}~2.21, ρ_{Ca}^{Li}~ 1.98	[128]
Simulated acidic brine	50	50	50	50	50	Imprinted CDI	ρ_{Na}^{Li}~6.32, ρ_{K}^{Li}~11.52, ρ_{Mg}^{Li}~13.52	[144]

(Note: "–" indicates that the corresponding ion concentration was not reported in the original publication; "/" denotes that the respective ion was not present in the feed solution.)

Table 4
Representative studies employing natural brines for Li recovery via CDI. The table summarizes the major cation concentrations and corresponding Li selectivity factors reported in each case. Note that CDI system configurations vary across studies.

Natural brine	Cation concentration (mg/L)					Selectivity factor				Ref.
	Li	Na	K	Mg	Ca	Li/Na	Li/K	Li/Mg	Li/Ca	
Dongtaijinaier salt lake	93.6	15,117.2	1578.0	2729.5	102.0	19.1	3.6	32.9	0.9	[114]
Tibet salt lake	295.35	20,997	2958	2524	213.81	116.88	136.11	187.50	4.92	[109]
						2.21	1.65	1.59	1.78	[162]
Golmud salt lake	1065.8	2020.5	982.2	84,553.4	3738.6	4.04	2.37	6307.19	1471.68	[163]
	1299	1886	719.75	47,000	4657.5	/	/	4.13–24.94	/	[159]
Zabuye salt lake	605	50,540	6250	54	112	513	212	804	/	[118]
East-Taijinaier Salt lake	50	80	20	1200	–	7.0	11.1	53.8	/	[125]
Lop Nor Xieli salt flat	42.09	95,366.54	10,101.31	29,403.1	57.71	6.8	4.2	2.0	2.5	[164]
Poland geothermal brine	15.7	10,298	102.1	50.3	63.7	5.6	5.5	4.4	1.3	[168]
	12.6	7363	80	38.2	57.6	4.6	3.8	2.5	3.2	[169]

(Note: "–" indicates that the corresponding ion concentration was not reported in the original publication; "/" denotes that the metric was not present in the original publication.)

section provides a comprehensive overview of the key metrics employed in the literature, summarizes their calculation approaches, highlights differences and limitations, and offers recommendations for future standardization.

4.2.1. Lithium adsorption capacity

Lithium adsorption capacity (LAC or Q_{Li}), also referred to lithium adsorption amount, is the most widely used metric to quantify the amount of lithium ions removed per unit mass of electrode material. It is typically calculated using the following formulas:

$$LAC\ or\ Q_{Li} = \frac{\left(C_0^{Li} - C_e^{Li}\right)V_0}{m} \tag{1}$$

$$LAC\ or\ Q_{Li} = \frac{\left|C_0^{Li}\mathrm{V}_0 - C_e^{Li}\mathrm{V}_e\right| - \sum_0^t C_t^{Li}\mathrm{V}_t}{m} \tag{2}$$

Where C_0^{Li}, C_e^{Li}, and C_t^{Li} (mol/L or mg/L) represent the lithium concentrations in the feed solution, the final effluent, and at time t in the CDI adsorption phase, respectively; V_0, V_e, and V_t (L) denote the volume of feed solution, final effluent, and the collected sample at time t; m (g) is

the mass of the electrode or the effective material mass on the electrode. Eq. (1) is applicable when no solution samples are collected during the electrosorption process, while Eq. (2) accounts for the loss of solution volume due to intermittent sampling. However, to simplify calculations, many studies adopt Eq. (1) and neglect the effect of collected sample volumes on the final result.

While simple and intuitive, this method varies across studies in terms of what is defined as active material (e.g., total electrode weight vs. active phase only), leading to inconsistencies. Some researchers also report capacity normalized to geometric electrode area (mg/cm^2), which complicates direct comparison. In addition, some investigations focus exclusively on the adsorption phase, reflecting lithium removal rather than recovery potential [99]. Conversely, certain studies also calculate desorption metrics independently, further complicating comprehensive evaluation [31,147].

Desorption efficiency (D) or the recovery rate (RR) were employed to evaluate the proportion of desorbed lithium relative to the initially adsorbed lithium. These are typically calculated using the following equation:

$$D \text{ or } RR\ (\%) = \frac{\left(C_{de}^{Li} - C_{d0}^{Li}\right) V_d}{\left(C_0^{Li} - C_e^{Li}\right) V_0} \times 100\% \tag{3}$$

Where C_{d0}^{Li} and C_{de}^{Li} (mol/L or mg/L) are the lithium concentrations in the initial desorption solution and the final effluent in the CDI desorption phase, respectively. V_d (L) is the volume of desorption solution.

4.2.2. Separation metrics

Selectivity is a critical parameter for quantifying the preference of electrodes for lithium over competing cations such as Na^+, K^+, Mg^{2+}, and Ca^{2+} in multicomponent systems. Two main approaches have been adopted in the literature to quantify selectivity, each offering different insights into ion discrimination mechanisms.

The first method is the adsorption selectivity ratio ρ_M^{Li}, which reflects the relative efficiency of lithium compared to a competing ion M, and is defined as:

$$\rho_M^{Li} = \frac{\eta_{Li}}{\eta_M} \tag{4}$$

Where η_x is the ion removal efficiency (or adsorption rate) given by:

$$\eta_x = \frac{C_0^x - C_e^x}{C_0^x} \times 100\% \tag{5}$$

Where C_0^x and C_e^x are the initial and final concentrations of ion x during the CDI adsorption phase.

This method is widely used in batch-mode or flow-through CDI tests with synthetic brines, as it provides a simple means to compare the extent of lithium removal against other ions under the same experimental conditions. However, this method is highly sensitive to the concentration of background ions. Elevated competing ion levels can suppress lithium uptake, leading to underestimated selectivity ratios. Moreover, it does not account for desorption behavior and is limited to the adsorption phase.

The second method is the separation factor S_M^{Li}, which captures the relative enrichment of lithium in the desorption effluent compared to the competing ion, and is expressed as:

$$S_M^{Li} = \frac{C_{de}^{Li} / C_{de}^{M}}{C_0^{Li} / C_0^{M}} \tag{6}$$

Where C_0^M and C_{de}^M are the concentrations of M in the feed solution and the final effluent in the CDI desorption phase, respectively. This metric is especially valuable in closed-loop or regeneration-focused studies, as it reflects the potential of selective lithium recovery during desorption. However, values of S_M^{Li} are highly dependent on desorption solution composition, desorption time, and prior adsorption loading. Some recent studies attempt to report both ρ_M^{Li} and S_M^{Li} concurrently, providing a more holistic view of CDI selectivity. However, few studies have benchmarked these metrics under standardized test conditions, e.g., fixed Li^+/M^+ ratio, identical operating voltage, or real brine matrices, limiting direct comparison across materials and configurations. Thus, while both methods provide useful insight into lithium selectivity, their interpretation must be contextualized within experimental design, ionic background, and phase of evaluation. Future studies should report both metrics under standardized conditions or provide normalization strategies to facilitate comparison.

4.2.3. Charge efficiency and energy consumption

Charge efficiency Λ quantifies the fraction of the total applied charge that is effectively used for lithium adsorption, serving as an indicator of electrochemical utilization. Its calculations may differ markedly depending on whether they account for total ion removal, lithium-specific recovery, or are based on idealized theoretical capacities derived from electrochemical characterizations such as cyclic voltammetry (CV) rather than actual CDI cell experiments. CDI-based charge efficiency is calculated as:

$$\Lambda = \frac{\left(C_t^{Li} - C_0^{Li}\right) V_0 F}{M_{Li} Q} \times 100\% \tag{7}$$

Where F is the Faraday constant (96,485C mol^{-1}); M_{Li} is the molar mass of Li (6.94 g mol^{-1}); Q (C) is the charge supplied per adsorption cycle. A higher charge efficiency indicates that a greater proportion of input electrical energy contributes to targeted lithium capture rather than parasitic reactions. However, Λ is highly sensitive to side reactions such as water electrolysis, especially at higher voltages or in real brine matrices with redox-active impurities. Moreover, discrepancies in the definition of Q, e.g., total charge passed vs. effective charge after background correction, lead to inconsistencies in reported values across studies. Few papers account for coulombic losses or correct for baseline current, resulting in overestimated efficiencies.

In parallel, energy efficiency is often evaluated using the energy normalized to lithium (ENL), which reflects the number of lithium moles captured per joule of energy consumed. It is defined as:

$$\text{ENL}\ (\mu\text{mol/J}) = \frac{\left(C_t^{Li} - C_0^{Li}\right) V_0}{\text{M}_{\text{Li}} \text{E}_{\text{ad}}} = \frac{\left(C_t^{Li} - C_0^{Li}\right) \int \text{Idt}}{\text{M}_{\text{Li}}} \tag{8}$$

Where E_{ad} is the energy supplied during CDI process, and $\int$ Idt is the time-integrated current over the cycle. ENL is particularly useful for comparing different CDI system designs or operational modes under practical energy constraints. Despite its importance, ENL remains underreported in the literature, partly due to the difficulty of accurately measuring instantaneous power and integrating it over dynamic CDI cycles. Only a few studies have systematically correlated ENL with lithium recovery efficiency and selectivity [19,59]. Additionally, different energy measurement methods further complicated interpretation.

4.2.4. Electrosorption kinetics

Adsorption and desorption kinetics are key indicators of the operational efficiency of CDI systems. Rapid adsorption kinetics enable high-throughput processing and facilitate continuous or semi-continuous operation, which are critical for practical deployment in lithium extraction. Faster kinetics enable shorter cycle times, lower energy consumption per unit lithium recovered, and improved compatibility with continuous-flow operations. Kinetic performance is commonly assessed using either empirical rate metrics or model-based fitting approaches.

A widely used empirical metric is the average electrosorption rate (AESR), which reflects the lithium removal rate normalized to either

electrode mass or area over a defined period. It is expressed as:

$$AESR = \frac{(C_0^{Li} - C_t^{Li})V_0}{mt} \quad (9)$$

However, AESR is dependent on test duration and initial concentration, and may overestimate performance if calculated before equilibrium is reached. In equilibrium-based batch adsorption experiments, kinetic behavior is often described by fitting adsorption data to classical models [129,144]. The pseudo-first-order (PFO) model assumes that the adsorption rate is proportional to the number of unoccupied sites, and is described as:

$$\frac{dq_t}{dt} = k_1(q_e - q_t) \quad (10)$$

The pseudo-second-order (PSO) model, which often provides a better fit for chemisorption-driven or intercalation-dominated processes, assumes the adsorption rate is proportional to the square of the unoccupied sites:

$$\frac{dq_t}{dt} = k_1(q_e - q_t)^2 \quad (11)$$

Where q_t and q_e are the adsorption capacities at time t and at equilibrium, respectively, and k_1, k_2 are rate constants. The choice of model depends on electrode properties and adsorption mechanisms. PSO models generally provide a better fit for ion-imprinted polymer systems and LIS-based electrodes. In contrast, porous carbon-based electrodes tend to follow PFO kinetics, especially when surface adsorption dominates. Nonetheless, fitting accuracy is often limited by sparse time-point sampling and the neglect of intra-particle diffusion or film resistance effects. Moreover, the kinetic models are primarily derived from batch adsorption systems and may not accurately represent real-time CDI dynamics, particularly under constant current or voltage modes.

Desorption kinetics are often overlooked but are equally critical for evaluating full-cycle recovery. Slow or incomplete desorption can lead to capacity fading, electrode passivation, and increased energy demands in successive cycles. Despite its importance, desorption kinetics are rarely quantified, and no standard metric currently exists for benchmarking regeneration speed.

4.2.5. Regeneration and cycling stability

Cycling stability is crucial to assessing the long-term reliability of CDI electrodes. It reflects the electrode's ability to maintain performance over repeated electrosorption–desorption cycles under operational conditions. Key indicators include capacity retention (CR), lithium selectivity retention (SR), and material integrity over time. CR and SR are defined as:

$$CR = \frac{Q_n}{Q_1} \times 100\% \quad (12)$$

$$SR = \frac{S_n^{Li/M}}{S_1^{Li/M}} \times 100\% \quad (13)$$

Where Q_1 and Q_n are the LAC in the first and n^{th} cycle, respectively; $S_1^{Li/M}$ and $S_n^{Li/M}$ are the lithium selectivity in the first and n^{th} cycle, respectively.

The degradation may arise from several mechanisms, including electrode material dissolution or leaching, structural collapse or loss of ion-accessible surface area due to repeated swelling/shrinkage, and accumulation of irreversible co-ions or impurities on the electrode surface. Most studies report cycling data over 10 to 100 cycles, but the test conditions such as regeneration method, applied voltage, and electrolyte composition vary substantially, impeding cross-study comparison. Cycling performance is often underreported or assessed under mild, idealized conditions that do not reflect real-world brine compositions. Long-term testing in complex feed matrices is critical for commercial viability.

Methodological discrepancies also arise from different analytical measurement approaches. Some studies use direct CDI testing with coupled plasma mass spectrometry (ICP-MS) analysis of effluents to evaluate real-time lithium recovery and cycling behavior [98,118,126,162]. Others rely on electrochemical proxy measurements such as CV, electrochemical impedance spectroscopy (EIS), and galvanostatic charge–discharge (GCD) in three-electrode setups [109,143,155]. Such electrochemical proxy results, while insightful at a mechanistic level, may not accurately reflect practical CDI performance due to differences in system conditions, electrode arrangements, and ion transport dynamics. Cycle stability testing further amplifies discrepancies, with metrics derived from different cycling protocols ranging from single-cycle assessments [100,147] to multi-cycle average results [98,109,111,162]. Given the significance of electrode stability and potential performance degradation due to electrode aging, fouling, and ion-exchange equilibrium changes, these varied protocols significantly impact reported outcomes.

4.3. Recommendations for standardization

To enable meaningful comparison and accelerate progress in CDI-based lithium recovery, the adoption of standardized performance evaluation protocols is essential. Currently, variations in feed solution compositions, testing durations, operational modes, and metric definitions, e.g., adsorption capacity, selectivity, or energy consumption, hinder the direct comparison of results across studies. Without standardized protocols, reported performances may reflect differences in experimental design rather than true material or process advantages. Establishing uniform testing procedures and clearly defined metrics will ensure comparability, improve reproducibility, and facilitate objective benchmarking of CDI systems for lithium recovery. In particular, studies should clearly report feed solution compositions, including lithium concentration, concentrations of major competing ions (e.g., Na^+, K^+, Mg^{2+}, and Ca^{2+}), as well as key ion ratios such as Li/Mg and Li/Na that strongly influence lithium selectivity. Given the diversity of feed solution types, metric selection and measurement methods should be tailored accordingly.

For binary or simplified systems, studies should report lithium-specific adsorption–desorption capacities, cycle-averaged selectivity factors using unified formulae, and consistent energy efficiency metrics over multiple cycles. Experimental conditions such as applied voltage, cycle duration, electrode mass loading, and solution volume should also be clearly specified to allow reproducibility and fair comparison across studies. For multi-ion synthetic and real brines, standardized ICP-based ion concentration measurements across repeated cycles are critical. Metrics must integrate both adsorption and desorption contributions to reflect true lithium recovery.

Across all systems, key parameters, such as LAC, selectivity, charge efficiency, ENL, and kinetic rates, should follow consistent definitions with clearly stated normalization bases. Cycling tests under realistic conditions should be conducted, reporting the retention of both capacity and selectivity. Where possible, testing using simulated multi-ion brines or representative natural brines is recommended in addition to simplified single-salt systems to better reflect practical lithium recovery conditions. Electrochemical proxy results are suggested to be clearly distinguished from CDI-derived data.

5. Challenges and future perspectives

5.1. Challenges

Despite the significant progress in CDI-based lithium recovery, several challenges remain before the technology can be translated from laboratory-scale studies to practical applications. One major challenge lies in the development of electrode materials that combine high lithium

selectivity, fast ion transport kinetics, and long-term cycling stability. Although various lithium-ion sieves, redox-active materials, MOF-derived structures, and carbon-based composites have demonstrated promising performance, many of these materials remain at the proof-of-concept stage. Further research is needed to improve structural stability, suppress competing ion interference, and enhance electrochemical durability under realistic operating conditions. Additionally, most current studies primarily focus on the design of lithium-selective working electrodes, while the role of counter electrodes has received comparatively limited attention. In typical CDI-based lithium recovery systems, activated carbon or ion-exchange-membrane-coated carbon electrodes are commonly used as counter electrodes to provide charge compensation. However, the electrochemical properties of the counter electrode can significantly influence system stability, energy efficiency, and overall lithium recovery performance.

Beyond material-related challenges, several system-level issues must also be addressed. Real brine compositions typically contain high concentrations of competing ions such as Na^{+}, Mg^{2+}, Ca^{2+}, and K^{+}, which can significantly reduce lithium selectivity and affect electrode stability during long-term operation. In addition, the presence of suspended solids, organic matter, or scaling species in practical water matrices may lead to fouling and performance deterioration in CDI systems. Furthermore, energy efficiency and operational optimization remain critical considerations. Although CDI generally operates at relatively low voltages, the overall energy consumption is strongly influenced by operational parameters such as applied voltage, flow rate, cycle duration, and electrode utilization.

Another critical issue is the lack of standardized evaluation methodologies across CDI studies. Current research employs a wide variety of feed solution compositions, testing conditions, and performance metrics, which complicates the direct comparison of reported results. In particular, simplified single-ion or binary solutions are often used to demonstrate lithium selectivity, whereas practical brine systems contain complex mixtures of competing ions. This lack of methodological consistency limits the ability to fairly benchmark materials and CDI configurations across different studies.

5.2. *Future perspectives*

To advance CDI-based lithium recovery toward practical implementation, future research should focus on both material innovation and system-level optimization. From a materials perspective, further development of lithium-selective electrode materials with improved structural stability, faster ion transport pathways, and enhanced resistance to competing ions will be essential. In addition, the coordinated design of both working and counter electrodes should be considered to ensure balanced electrochemical performance. Rational capacity matching between electrodes may help improve charge utilization, energy efficiency, and long-term operational stability. Future studies should also emphasize the adoption of standardized testing protocols. Experiments conducted under representative multi-ion brine conditions, combined with consistent definitions of key performance metrics such as lithium adsorption capacity, selectivity factors, charge efficiency, and energy consumption, will enable more meaningful comparisons across different CDI systems and materials.

In addition, the scalability and system integration of CDI technologies remain important research directions. Most current studies are conducted using small laboratory cells with limited electrode areas and batch operation modes, which differ significantly from practical industrial systems. Translating laboratory-scale CDI configurations into practical lithium extraction systems requires improvements in electrode manufacturing, module design, and long-term operational stability. The integration of CDI with complementary technologies, such as membrane separation or electrochemical processes, may also provide opportunities to enhance lithium recovery efficiency. Future scale-up strategies may include the development of modular CDI stacks with enlarged electrode areas, optimization of flow distribution within multi-cell modules, and the integration of continuous-flow operation. In addition, scalable electrode fabrication methods and durable materials capable of maintaining performance over long-term cycling will be essential for practical deployment. Addressing these engineering challenges will be crucial for translating CDI-based lithium recovery from laboratory demonstrations to industrial-scale applications.

6. Conclusions

CDI has emerged as a promising technology for lithium recovery from low-grade and compositionally complex aqueous resources. Compared to conventional extraction methods, CDI offers advantages such as low energy consumption, mild operating conditions, and electrode regenerability. Recent advances in electrode materials, structural engineering, and system configurations have significantly improved lithium adsorption capacity and selectivity. Continued progress in CDI-based lithium recovery will depend on the combined development of advanced electrode materials, improved system designs, and standardized evaluation methodologies. With ongoing research efforts and improved understanding of ion-selective mechanisms, CDI has strong potential to become a viable technology for sustainable lithium extraction from unconventional aqueous resources.

CRediT authorship contribution statement

Hanwei Yu: Conceptualization, Data curation, Formal analysis, Investigation, Methodology, Writing – original draft. **Sherub Phuntsho:** Conceptualization, Formal analysis, Project administration, Resources, Supervision, Validation, Writing – review & editing. **Gayathri Naidu:** Formal analysis, Funding acquisition, Project administration, Writing – review & editing. **Mohsen Askari:** Investigation, Writing – review & editing. **Ho Kyong Shon:** Conceptualization, Data curation, Formal analysis, Funding acquisition, Investigation, Methodology, Project administration, Resources, Supervision, Validation, Writing – review & editing.

Declaration of competing interest

The authors declare the following financial interests/personal relationships which may be considered as potential competing interests: The authors declare that they have no known competing financial interests or personal relationships that could have appeared to influence the work reported in this research paper. Professor Ho Kyong Shon serves as a co-Editor-in-Chief for the Desalination journal, while the editorial handling and review of this manuscript were overseen by a different Editor.

Acknowledgments

We thank financial support from the Australian Research Council (ARC) Discovery Projects (DP230100238).

Data availability

Data will be made available on request.

References

[1] H. Yu, et al., Metal-based adsorbents for lithium recovery from aqueous resources, Desalination 539 (2022) 115951.
[2] LithiumHarvest, *Discover the booming lithium market driven by EVs and renewable energy as demand surges and supply chains evolve*, in *The Lithium Mining Market*, 2025.
[3] V. Balaram, et al., Lithium: a review of applications, occurrence, exploration, extraction, recycling, analysis, and environmental impact, Geosci. Front. 15 (2024) 101868.

[4] LithiumHarvest, *Discover the different lithium extraction methods: exploring greener alternatives and the game-changing technology of Lithium Harvest*, in *Lithium Extraction Methods*, 2025.
[5] A. Persson, Understand lithium Mining's Environmental Impact, Carbon Chain, 2024.
[6] Z. Xu, et al., Predicting the performance of lithium adsorption and recovery from unconventional water sources with machine learning, Water Res. 266 (2024) 122374.
[7] H. Qian, et al., HTO/cellulose aerogel for rapid and highly selective Li^+ recovery from seawater, Molecules 26 (2021) 4054.
[8] L. Kong, et al., Electro-driven direct lithium extraction from geothermal brines to generate battery-grade lithium hydroxide, Nat. Commun. 16 (1) (2025) 806.
[9] S. Yang, et al., Lithium extraction from low-quality brines, Nature 636 (8042) (2024) 309–321.
[10] A. Khalil, et al., Lithium recovery from brine: recent developments and challenges, Desalination 528 (2022) 115611.
[11] D.Y. Butylskii, et al., Review of recent progress on lithium recovery and recycling from primary and secondary sources with membrane-based technologies, Desalination 586 (2024) 117826.
[12] N. Pathak, et al., Membrane technology for brine management and valuable resource recovery, in: Green Membrane Technologies towards Environmental Sustainability, 2023, pp. 415–441.
[13] D.Y. Butylskii, et al., Selective recovery of lithium ion from its mixed solution with potassium and sodium by electrobaromembrane method, Sep. Purif. Technol. 343 (2024) 126675.
[14] D. Jiang, et al., Insights into electrochemical paradigms for lithium extraction: electrodialysis versus capacitive deionization, Coord. Chem. Rev. 516 (2024) 215923.
[15] H. Lee, et al., Sustainable approach for selective lithium recovery: capacitive deionization integrated with novel LMO flow-electrode, Desalination 593 (2025) 118224.
[16] L. Miao, et al., Progress toward adsorption mechanism exploration method for capacitive deionization: experimental, mathematical model, computational chemistry and machine learning, Desalination 586 (2024) 117850.
[17] Z. He, et al., Membrane capacitive deionization (MCDI): a flexible and tunable technology for customized water softening, Water Res. 259 (2024) 121871.
[18] X. Zhang, et al., Selective ion separation by capacitive deionization (CDI) based technologies: a state-of-the-art review, Environ. Sci. Water Res. Technol. 6 (2) (2020) 243–257.
[19] H. Yu, et al., Selective lithium extraction from diluted binary solutions using metal-organic frameworks (MOF)-based membrane capacitive deionization (MCDI), Desalination 556 (2023) 116569.
[20] S.M. Hossain, et al., ZiF-8 induced carbon electrodes for selective lithium recovery from aqueous feed water by employing capacitive deionization system, Desalination 546 (2023) 116201.
[21] R. Kumar, et al., Sustainable lithium extraction from liquid ores using membrane-based technologies: a review, Environ. Chem. Lett. 23 (2025) 1569–1660.
[22] J. Park, et al., Electrochemical direct Lithium extraction: a review of Electrodialysis and capacitive deionization technologies, Resources 14 (2) (2025).
[23] L. Wu, et al., Lithium recovery using electrochemical technologies: advances and challenges, Water Res. 221 (2022) 118822.
[24] H. Yuan, et al., Electrochemical extraction technologies of lithium: development and challenges, Desalination 598 (2025) 118419.
[25] Y. Zhou, et al., Research Progress of Technology of lithium Extraction, Sep. Purif. Technol. 359 (2025) 130561.
[26] J. Farahbakhsh, et al., Direct lithium extraction: a new paradigm for lithium production and resource utilization, Desalination 575 (2024) 117249.
[27] T.M. Khoi, et al., Recent advances in selective ion separation using flow-electrode capacitive deionization, Desalination 617 (2026) 119429.
[28] J. Wang, et al., Capacitive deionization in water treatment: a review of reactor dynamics, electrode materials, functional membranes, and modeling techniques, Desalination 600 (2025) 118459.
[29] M. Askari, et al., Advances in capacitive deionization (CDI) systems for nutrient recovery from wastewater: paving the path towards a circular economy, Desalination 583 (2024) 117695.
[30] T. Pang, et al., Advances and challenges in capacitive deionization: materials, architectures, and selective ion removal, Desalination 592 (2024) 118140.
[31] H. Yu, et al., Integrated sulfonated poly ether ketone membrane capacitive deionization for lithium recovery from diluted binary solutions, Sep. Purif. Technol. 352 (2025).
[32] J. Si, et al., Selective membrane capacitive deionization for superior lithium recovery, Desalination 572 (2024) 117154.
[33] T.M. Khoi, et al., Selective and continuous ion recovery using flow electrode capacitive deionization with polymer multilayers functionalized ion exchange membrane, Desalination 558 (2023) 116626.
[34] W. Shi, et al., Efficient lithium extraction by membrane capacitive deionization incorporated with monovalent selective cation exchange membrane, Sep. Purif. Technol. 210 (2019) 885–890.
[35] Y. Wang, et al., Selective ion separation in electrosorption systems: progress in material development and mechanism exploration, Chem. Commun. (Camb.) 61 (2025) 16686–16700.
[36] M.E. Suss, et al., Water desalination via capacitive deionization: what is it and what can we expect from it? Energy Environ. Sci. 8 (8) (2015) 2296–2319.
[37] M. Bryjak, et al., Capacitive deionization for selective extraction of lithium from aqueous solutions, Journal of Membrane and Separation Technology 4 (2015) 110–115.
[38] S. Porada, et al., Review on the science and technology of water desalination by capacitive deionization, Prog. Mater. Sci. 58 (8) (2013) 1388–1442.
[39] Z.-H. Huang, et al., Carbon electrodes for capacitive deionization, J. Mater. Chem. A 5 (2) (2017) 470–496.
[40] F. Duan, et al., Desalination stability of capacitive deionization using ordered mesoporous carbon: effect of oxygen-containing surface groups and pore properties, Desalination 376 (2015) 17–24.
[41] P.M. Biesheuvel, A. van der Wal, Membrane capacitive deionization, J. Membr. Sci. 346 (2) (2010) 256–262.
[42] A. Hassanvand, et al., A comparison of multicomponent electrosorption in capacitive deionization and membrane capacitive deionization, Water Res. 131 (2018) 100–109.
[43] Y. Zhao, et al., Performance comparison and energy consumption analysis of capacitive deionization and membrane capacitive deionization processes, Desalination 324 (2013) 127–133.
[44] F. Yang, et al., Flow-electrode capacitive deionization: a review and new perspectives, Water Res. 200 (2021) 117222.
[45] C. Zhang, et al., Flow electrode capacitive deionization (FCDI): recent developments, environmental applications, and future perspectives, Environ. Sci. Technol. 55 (8) (2021) 4243–4267.
[46] Z. Chen, et al., Ultra-durable and highly-efficient hybrid capacitive deionization by MXene confined MoS_2 heterostructure, Desalination 528 (2022) 115616.
[47] S. Dahiya, A. Singh, B.K. Mishra, Capacitive deionized hybrid systems for wastewater treatment and desalination: a review on synergistic effects, mechanisms and challenges, Chem. Eng. J. 417 (2021) 128129.
[48] S. Sahin, et al., Enhanced monovalent over divalent cation selectivity with polyelectrolyte multilayers in membrane capacitive deionization via optimization of operational conditions, Desalination 522 (2022) 115391.
[49] A. Hassanvand, et al., The role of ion exchange membranes in membrane capacitive deionisation, Membranes (Basel) 7 (3) (2017).
[50] P.A. Fritz, et al., Exergy analysis of membrane capacitive deionization (MCDI), Desalination 444 (2018) 162–168.
[51] J.-B. Lee, et al., Desalination of a thermal power plant wastewater by membrane capacitive deionization, Desalination 196 (1–3) (2006) 125–134.
[52] R. Zhao, P.M. Biesheuvel, A. van der Wal, Energy consumption and constant current operation in membrane capacitive deionization, Energy Environ. Sci. 5 (11) (2012).
[53] Y.-J. Kim, J.-H. Choi, Enhanced desalination efficiency in capacitive deionization with an ion-selective membrane, Sep. Purif. Technol. 71 (1) (2010) 70–75.
[54] R. Zhao, et al., Optimization of salt adsorption rate in membrane capacitive deionization, Water Res. 47 (5) (2013) 1941–1952.
[55] Z. He, et al., Optimization of constant-current operation in membrane capacitive deionization (MCDI) using variable discharging operations, Water Res. 204 (2021) 117646.
[56] H. Yoon, et al., Effects of characteristics of cation exchange membrane on desalination performance of membrane capacitive deionization, Desalination 458 (2019) 116–121.
[57] M. Wang, et al., Enhanced desalination performance of anion-exchange membrane capacitive deionization via effectively utilizing cathode oxidation, Desalination 443 (2018) 221–227.
[58] D.I. Kim, et al., Palladium recovery through membrane capacitive deionization from metal plating wastewater, ACS Sustain. Chem. Eng. 6 (2) (2017) 1692–1701.
[59] R. McNair, et al., Ionic covalent organic nanosheet (iCON)–quaternized polybenzimidazole nanocomposite anion-exchange membranes to enhance the performance of membrane capacitive deionization, Desalination 533 (2022) 115777.
[60] N.C. Nnorom, et al., Sulfonated polymer coating enhances selective removal of calcium in membrane capacitive deionization, J. Membr. Sci. 662 (2022) 120974.
[61] N. Kim, et al., Parametric investigation of the desalination performance in multichannel membrane capacitive deionization (MC-MCDI), Desalination 503 (2021) 114950.
[62] Q. Wu, et al., Novel inorganic integrated membrane electrodes for membrane capacitive deionization, ACS Appl. Mater. Interfaces 13 (39) (2021) 46537–46548.
[63] D. Ma, Y. Wang, Structure and process optimization for highly-efficient membrane capacitive deionization, Energ. Technol. 9 (4) (2021).
[64] Q. Wang, et al., Ammonia removal from municipal wastewater via membrane capacitive deionization (MCDI) in pilot-scale, Sep. Purif. Technol. 286 (2022) 120469.
[65] S.-i. Jeon, et al., Desalination via a new membrane capacitive deionization process utilizing flow-electrodes, Energy Environ. Sci. 6 (5) (2013).
[66] B. Kastening, T. Boinowitz, M. Heins, Design of a slurry electrode reactor system, J. Appl. Electrochem. 27 (1997) 147–152.
[67] F. Yu, et al., A comprehensive review on flow-electrode capacitive deionization: design, active material and environmental application, Sep. Purif. Technol. 281 (2022) 119870.
[68] L. Zhang, et al., Synthesis of biomass-derived N-doped carbon nanodots via a one-pot hydrothermal approach for enhanced lithium extraction in flow-electrode capacitive deionization, J. Environ. Chem. Eng. 13 (2025) 115677.
[69] S. Dsoke, et al., Strategies to reduce the resistance sources on electrochemical double layer capacitor electrodes, J. Power Sources 238 (2013) 422–429.
[70] S. Porada, et al., Carbon flow electrodes for continuous operation of capacitive deionization and capacitive mixing energy generation, J. Mater. Chem. A 2 (24) (2014).

[71] S. Dahiya, B.K. Mishra, Enhancing understandability and performance of flow electrode capacitive deionisation by optimizing configurational and operational parameters: a review on recent progress, Sep. Purif. Technol. 240 (2020) 116660.
[72] C. He, et al., Short-circuited closed-cycle operation of flow-electrode CDI for brackish water softening, Environ. Sci. Technol. 52 (16) (2018) 9350–9360.
[73] L. Xu, et al., Can flow-electrode capacitive deionization become a new in-situ soil remediation technology for heavy metal removal? J. Hazard. Mater. 402 (2021) 123568.
[74] C. Zhang, et al., Capacitive membrane stripping for Ammonia recovery (CapAmm) from dilute wastewaters, Environ. Sci. Technol. Lett. 5 (1) (2017) 43–49.
[75] J. Lee, et al., Hybrid capacitive deionization to enhance the desalination performance of capacitive techniques, Energy Environ. Sci. 7 (11) (2014) 3683–3689.
[76] W. Tang, et al., Various cell architectures of capacitive deionization: recent advances and future trends, Water Res. 150 (2019) 225–251.
[77] M.E. Suss, V. Presser, Water desalination with energy storage electrode materials, Joule 2 (1) (2018) 10–15.
[78] S. Kim, et al., Na2FeP2O7 as a novel material for hybrid capacitive deionization, Electrochim. Acta 203 (2016) 265–271.
[79] L. Guo, et al., A Prussian blue anode for high performance electrochemical deionization promoted by the faradaic mechanism, Nanoscale 9 (35) (2017) 13305–13312.
[80] S. Hand, R.D. Cusick, Characterizing the impacts of deposition techniques on the performance of MnO2 cathodes for sodium Electrosorption in hybrid capacitive deionization, Environ. Sci. Technol. 51 (20) (2017) 12027–12034.
[81] M. Tauk, et al., Ion-selectivity advancements in capacitive deionization: a comprehensive review, Desalination 572 (2024) 117146.
[82] M. Tauk, et al., Recent advances in capacitive deionization: a comprehensive review on electrode materials, J. Environ. Chem. Eng. 11 (6) (2023).
[83] L. Eliad, et al., Ion sieving effects in the electrical double layer of porous carbon electrodes estimating effective ion size in electrolytic solutions, J. Phys. Chem. B 105 (2001) 6880–6887.
[84] C.J. Gabelich, T.D. Tran, I.H. Suffet, Electrosorption of inorganic salts from aqueous solution using carbon aerogels, Environ. Sci. Technol. 36 (2002) 3010–3019.
[85] Y. Gao, et al., Electrosorption behavior of cations with carbon nanotubes and carbon nanofibres composite film electrodes, Thin Solid Films 517 (5) (2009) 1616–1619.
[86] L. Han, et al., Exploring the impact of pore size distribution on the performance of carbon electrodes for capacitive deionization, J. Colloid Interface Sci. 430 (2014) 93–99.
[87] M. Mossad, L. Zou, A study of the capacitive deionisation performance under various operational conditions, J. Hazard. Mater. 213-214 (2012) 491–497.
[88] S.J. Seo, et al., Investigation on removal of hardness ions by capacitive deionization (CDI) for water softening applications, Water Res. 44 (7) (2010) 2267–2275.
[89] L. Pilon, H. Wang, A. d`Entremont, Recent advances in continuum modeling of interfacial and transport phenomena in electric double layer capacitors, J. Electrochem. Soc. 162 (5) (2015) A5158–A5178.
[90] C. Zhang, et al., Faradaic reactions in capacitive deionization (CDI) - problems and possibilities: a review, Water Res. 128 (2018) 314–330.
[91] M.D. Radin, et al., Narrowing the gap between theoretical and practical capacities in Li-ion layered oxide cathode materials, Adv. Energy Mater. 7 (20) (2017).
[92] S. Sahin, et al., Modification of cation-exchange membranes with polyelectrolyte multilayers to tune ion selectivity in capacitive deionization, ACS Appl. Mater. Interfaces 12 (31) (2020) 34746–34754.
[93] Q. Cheng, et al., High specific surface crown ether modified chitosan nanofiber membrane by low-temperature phase separation for efficient selective adsorption of lithium, Sep. Purif. Technol. 262 (2021) 118312.
[94] M. Kazemabad, et al., Crown ether containing polyelectrolyte multilayer membranes for lithium recovery, J. Membr. Sci. 595 (2020) 117432.
[95] D. Ma, et al., Grafting the charged functional groups on carbon nanotubes for improving the efficiency and stability of capacitive deionization process, ACS Appl. Mater. Interfaces 11 (19) (2019) 17617–17628.
[96] P. Liu, et al., Grafting sulfonic and amine functional groups on 3D graphene for improved capacitive deionization, J. Mater. Chem. A 4 (14) (2016) 5303–5313.
[97] H. Zhang, et al., Ultrashort and vertically aligned channels: boosted Lithium selective extraction via hybrid capacitive deionization, Environ. Sci. Technol. 59 (13) (2025) 6881–6890.
[98] X. Shang, et al., CNT-strung LiMn(2) O(4) for Lithium extraction with high selectivity and stability, Small Methods 6 (7) (2022) e2200508.
[99] B. Hu, et al., Lithium ion sieve modified three-dimensional graphene electrode for selective extraction of lithium by capacitive deionization, J. Colloid Interface Sci. 612 (2022) 392–400.
[100] X. Shang, et al., Synthesis of lithium vanadate/reduced graphene oxide with strong coupling for enhanced capacitive extraction of lithium ions, Sep. Purif. Technol. 262 (2021) 118294.
[101] G. Bhaskaran, et al., Layered hydrated-titanium-oxide-laden reduced graphene oxide composite as a high-performance negative electrode for selective extraction of Li via membrane capacitive deionization, J. Colloid Interface Sci. 650 (Pt A) (2023) 752–763.
[102] Y. Wang, et al., Charged cyclodextrin membranes for precise molecular sieving, J. Mater. Chem. A 10 (41) (2022) 22301–22310.
[103] Z. Shao, et al., Crown ether-based covalent organic framework packed Nanofiltration membrane for efficient Mg(2+)/Li(+) ion sieving, ChemSusChem 18 (2025) e202501076.
[104] D. Lei, et al., Covalent organic framework membranes for lithium extraction: facilitated ion transport strategies to enhance selectivity, Mater. Horiz. 12 (15) (2025) 5459–5472.
[105] Y. Dong, et al., Crown ether-based Tröger's base membranes for efficient Li+/Mg2+ separation, J. Membr. Sci. 665 (2023) 121113.
[106] Y.-P. Tian, et al., Mechanism of Li+/Na+ separation by crown ether and butyrate acid root, Rare Metals 42 (4) (2023) 1238–1248.
[107] B. Hu, et al., Prussian blue analogue derived 3D hollow LiCoMnO4 nanocube for selective extraction of lithium by pseudo-capacitive deionization, Desalination 560 (2023) 116662.
[108] Y. Xu, et al., Selective extraction of lithium ion based on lithium iron phosphate flow electrode, Sep. Purif. Technol. 367 (2025) 132948.
[109] J. Zhou, et al., Highly selective lithium extraction from salt lake via carbon-coated lithium vanadium phosphate capacitive electrode, Chem. Eng. J. 482 (2024) 148985.
[110] Q. Li, et al., Faradaic electrodes open a new era for capacitive deionization, Adv. Sci. 7 (22) (2020) 2002213.
[111] M. Rethinasabapathy, et al., Efficient lithium extraction using redox-active Prussian blue nanoparticles-anchored activated carbon intercalation electrodes via membrane capacitive deionization, Chemosphere 336 (139256) (2023) 139256.
[112] J. Liu, et al., Alkaline resins enhancing Li^+/H^+ ion exchange for Lithium recovery from brines using granular titanium-type Lithium ion-sieves, Ind. Eng. Chem. Res. 60 (45) (2021) 16457–16468.
[113] G. Liao, et al., High selectivity, capacity and stability for electrochemical lithium extraction on boron-doped H(1.6)Mn(1.6)O(4) by tailoring lattice constant and intercalation energy, Water Res. 274 (2025) 123131.
[114] Y. Xu, et al., LiMn(2)O(4) nanoparticles in situ embedded in carbon networks for Lithium extraction from brine via hybrid capacitive deionization, ACS Appl. Mater. Interfaces 17 (3) (2025) 4821–4831.
[115] H. Yu, et al., Highly selective lithium recovery from seawater desalination brine using Li(2)TiO(3) membrane-coated capacitive deionization, Water Res. 285 (2025) 124113.
[116] Z. Guo, et al., Integrating FeOOH with bacterial cellulose-derived 3D carbon nanofiber aerogels for fast and stable capacitive deionization based on accelerating chloride insertion, Desalination 576 (2024) 117329.
[117] B. Xiao, et al., Bacterial cellulose: a versatile 3D nanostructure advancing electrode engineering for high-performance capacitive deionization, Desalination 612 (2025) 118955.
[118] S. Li, et al., Selective lithium extraction with LiMn2O4: impossible triangle and reconcile via in-situ growth on flexible 3D substrate, Sep. Purif. Technol. 351 (2024) 128131.
[119] C. Bourdiol, et al., Selective lithium recovery using electrochemical ion pumping for Li-ion battery recycling, Sep. Purif. Technol. 382 (2026) 135816.
[120] E.J. Calvo, Electrochemical methods for sustainable recovery of lithium from natural brines and battery recycling, Curr. Opin. Electrochem. 15 (2019) 102–108.
[121] J. Xiong, et al., Direct lithium extraction from raw brine by chemical redox method with LiFePO4/FePO4 materials, Sep. Purif. Technol. 290 (2022) 120789.
[122] E.J. Calvo, Direct Lithium recovery from aqueous electrolytes with electrochemical ion pumping and Lithium intercalation, ACS Omega 6 (51) (2021) 35213–35220.
[123] C. Li, et al., Constructing porous hydrophilic HMO/CTA@PDA composite hydrogel for super-high and ultrafast extraction of lithium ions, Desalination 593 (2025) 118216.
[124] E. Li, et al., Precisive lithium extraction based on synergistic effect of water-rich 3D network in hydrogel and covalent grafted crown ether, Desalination 617 (2026) 119411.
[125] W. Jin, et al., Simultaneous and precise recovery of lithium and boron from salt lake brine by capacitive deionization with oxygen vacancy-rich CoP/Co3O4-graphene aerogel, Chem. Eng. J. 420 (2021) 127661.
[126] G. Tan, et al., Reduced lattice constant in Al-doped LiMn(2)O(4) nanoparticles for boosted electrochemical lithium extraction, Adv. Mater. 36 (14) (2024) e2310657.
[127] B. Hu, et al., Go-encapsulated La-doped lithium manganese oxide assemblies to enhance lithium extraction performance in capacitive deionization, Sep. Purif. Technol. 348 (2024) 127693.
[128] J. Li, et al., Lithium extraction via capacitive deionization: AlF3 coated LiMn2O4 spheres for enhanced performance, Desalination 591 (2024) 118035.
[129] N. Han, et al., Selective recovery of lithium ions from acidic medium based on capacitive deionization-enhanced imprinted polymers, J. Clean. Prod. 373 (2022) 133773.
[130] S. Wang, et al., Enhanced Lithium adsorption on an anion- and cation-Codoped Lithium manganese oxide ion sieve with a thin fluoride-protective coating layer, Ind. Eng. Chem. Res. 63 (21) (2024) 9527–9537.
[131] T. Ryu, et al., Lithium recovery system using electrostatic field assistance, Hydrometallurgy 151 (2015) 78–83.
[132] V.P. Huynh, et al., Selective lithium separation from Li/co/Ni mixtures using optimized flow-electrode capacitive deionization, Desalination 592 (2024) 118112.
[133] D.-H. Lee, et al., Selective lithium recovery from aqueous solution using a modified membrane capacitive deionization system, Hydrometallurgy 173 (2017) 283–288.

[134] B. Han, et al., Thin and defect-free ZIF-8 layer assisted enhancement of the monovalent perm-selectivity for cation exchange membrane, Desalination 529 (2022).
[135] Y. Liu, et al., The application of Zeolitic imidazolate frameworks (ZIFs) and their derivatives based materials for photocatalytic hydrogen evolution and pollutants treatment, Chem. Eng. J. 417 (2021) 127914.
[136] G. Zhang, et al., Metal–organic framework derived micro−/nano-materials: precise synthesis and clean energy applications, Inorg. Chem. Front. 11 (19) (2024) 6275–6306.
[137] J. Qiao, et al., ZIF-8 derived carbon with confined sub-nanometer pores for electrochemically selective separation of chloride ions, Sep. Purif. Technol. 295 (2022) 121222.
[138] C. He, et al., Construction of hierarchical Zn-HHTP/LDH heterostructures for selective and enhanced lithium extraction via capacitive deionization, Desalination 618 (2026) 119490.
[139] C. He, et al., In situ engineering of conductive MOF/LDH heterojunction nanosheet arrays for high-efficiency lithium extraction via capacitive deionization, Chem. Eng. J. 523 (2025) 168530.
[140] Z.-W. Jiang, et al., Metal-organic framework/layered double hydroxide (MOF/LDH) hetero-nanosheet array for capacitive deionization, Chem. Eng. J. 502 (2024) 158120.
[141] J. Lim, et al., Capacitive deionization incorporating a fluidic MOF-CNT electrode for the high selective extraction of lithium, Desalination 578 (2024) 117403.
[142] L. Jiang, et al., Coupling hybrid membrane capacitive deionization (HMCDI) with electric-enhanced direct contact membrane distillation (EE-DCMD) for lithium/cobalt separation and concentration, Sep. Purif. Technol. 302 (2022) 122082.
[143] L. Bai, et al., Insights into adsorbent materials for lithium extraction by capacitive deionization: reconceptualizing the role of materials informatics, J. Mater. Chem. A 12 (18) (2024) 10676–10685.
[144] N. Han, et al., Adsorption of Li+ by imprinted capacitor deionization — a new method for selective recovery of valuable lithium in acidic solutions, Desalination 565 (2023) 116820.
[145] B. Yan, et al., Development and optimization of lithium-ion sieves through machine learning in complex brine systems, Sep. Purif. Technol. 374 (2025) 133726.
[146] H. Wang, et al., Advancement of capacitive deionization propelled by machine learning approach, Sep. Purif. Technol. 354 (2025) 129423.
[147] Q. Wang, et al., Electricity facilitates the lithium sorption from salt-lake brine by H3LiTi5O12 nanoparticles: kinetics, selectivity and mechanism, Chem. Eng. J. 471 (2023) 144532.
[148] S. Xu, et al., Extraction of lithium from Chinese salt-lake brines by membranes: design and practice, J. Membr. Sci. 635 (2021) 119441.
[149] M. Zheng, X. Liu, Hydrochemistry of salt lakes of the Qinghai-Tibet plateau, China, Aquat. Geochem. 15 (1–2) (2009) 293–320.
[150] Vi-Duang Dang, M. Steinberg, Preliminary design and analysis of recovery of lithium from brine with the use of a selective extractant, Energy 3 (1978) 325–336.
[151] A. Somrani, A.H. Hamzaoui, M. Pontie, Study on lithium separation from salt lake brines by nanofiltration (NF) and low pressure reverse osmosis (LPRO), Desalination 317 (2013) 184–192.
[152] J.W. An, et al., Recovery of lithium from Uyuni Salar brine, Hydrometallurgy 117-118 (2012) 64–70.
[153] P. Besson, et al., Calcium, Na, K and Mg concentrations in seawater by inductively coupled plasma-atomic emission spectrometry: applications to IAPSO seawater reference material, hydrothermal fluids and synthetic seawater solutions, Geostand. Geoanal. Res. 38 (3) (2014) 355–362.
[154] B. Kim, J.Y. Seo, C.-H. Chung, Electrochemical desalination and recovery of Lithium from saline water upon operation of a capacitive deionization cell combined with a redox flow battery, ACS EST Water 1 (4) (2021) 1047–1054.
[155] M. Faheem, et al., Recovery of lithium by pseudocapacitive electrodes in capacitive deionization, Electrochim. Acta 489 (2024) 144267.
[156] S. Bae, et al., Four-step constant voltage operation of hybrid capacitive deionization with composite electrodes for bifunctional deionization and lithium recovery, Desalination 565 (2023) 116883.
[157] X. Shang, et al., LiNi0.5Mn1.5O4-based hybrid capacitive deionization for highly selective adsorption of lithium from brine, Sep. Purif. Technol. 258 (2021) 118009.
[158] S. Roobavannan, et al., Selective lithium extraction using capacitive deionization with fabricated zeolitic imidazolate framework encapsulated manganese oxide carbon electrode, Chem. Eng. J. 483 (2024) 149242.
[159] G. Ma, et al., Lithium extraction from salt lake via rocking-chair flow electrode capacitive deionization with monovalent selective membrane, Desalination 600 (2025) 118516.
[160] Y. Ha, et al., Continuous Lithium extraction from aqueous solution using flow-electrode capacitive deionization, Energies 12 (15) (2019).
[161] A. Siekierka, M. Bryjak, Novel anion exchange membrane for concentration of lithium salt in hybrid capacitive deionization, Desalination 452 (2019) 279–289.
[162] G. Ma, et al., Binder-free LiMn(2) O(4) nanosheets on carbon cloth for selective lithium extraction from brine via capacitive deionization, Small 20 (9) (2024) e2306530.
[163] G. Ma, et al., Lithium extraction from salt lake brine by four-stage ion-distillation of flow electrode capacitive deionization, Chem. Eng. J. 493 (2024) 152519.
[164] Y. Bao, et al., Li-ions pre-intercalation strategy of manganese oxides for capacitive deionization-based selective lithium extraction from low-grade brine, Small (2024) e2406951.
[165] H.M. Saif, J.G. Crespo, S. Pawlowski, Lithium recovery from brines by lithium membrane flow capacitive deionization (Li-MFCDI) – a proof of concept, Journal of Membrane Science Letters 3 (2023) 100059.
[166] N. Xie, et al., Fabricating a flow-through hybrid capacitive deionization cell for selective recovery of Lithium ions, ACS Appl. Energy Mater. 4 (11) (2021) 13036–13043.
[167] T. Elmakki, et al., Capacitive lithium capture system using a mixed LiMn2O4 and LiAlO2 material, Desalination 593 (2025) 118195.
[168] A. Siekierka, M. Bryjak, Selective sorbents for recovery of lithium ions by hybrid capacitive deionization, Desalination 520 (2021) 115324.
[169] A. Siekierka, Lithium and magnesium separation from brines by hybrid capacitive deionization, Desalination 527 (2022) 115569.